VARIABILITY IN BEACH TOPOGRAPHY AND FORCING
ALONG OAK ISLAND, NORTH CAROLINA

Jesse H. Baldwin

A Thesis Submitted to the
University of North Carolina Wilmington in Partial Fulfillment
of the Requirements for the Degree of
Master of Science

Department of Geography and Geology

University of North Carolina Wilmington

2008

Approved by

Advisory Committee

Gregg Snedden | Jesse McNinch

Nancy Grindlay | Lynn Leonard
Chair

Accepted by

DN: cn=Robert D. Roer, o=UNCW, ou=Dean of the Graduate School & Research, email=roer@uncw.edu, c=US
Date: 2009.04.14 20:59:48 -04'00'
Robert Roer

Dean, Graduate School

This thesis has been prepared in a style and format

consistent with

Estuarine, Coastal and Shelf Science

.

TABLE OF CONTENTS

ABSTRACT

This study analyzed variability in beach topography along Oak Island, North Carolina as well as local wave, water level, and wind conditions over a two year period to identify patterns of variability in shoreline change and potential processes forcing these patterns. Empirical Orthogonal Function (EOF) analysis was used to identify dominant modes of variability in beach topography along the western 17 km of Oak Island between June 2004 and June 2006. This analysis allows identification of separate patterns of variability in time series data, each with a specific spatial and temporal signature, and each explaining a specific percent of variance in the data. Kinematic GPS was used to collect beach topography data bimonthly at 12 shore-perpendicular beach profile transects (dune to MLW) spaced at 0.5 - 2.0 km intervals along the beach. The EOF analysis was then performed on a vectorized time series of beach surface elevations for the entire study reach measured during the 13 separate surveys to identify both cross-shore and along-shore variability. Wave, water level and wind data were compiled from a number of local stations to identify potential processes forcing shoreline variability. A number of averaging windows were applied to these parameters ranging from one day before each survey to the entire period between surveys. These parameters were then correlated against each mode to identify significant relationships and determine whether these processes were more important over shorter or longer time periods before each survey. Results of the EOF analysis include two dominant patterns of variability in beach topography which combine to explain 63% of all variability in the data. The first mode, explaining 44% of variance in the time series, showed large scale shoreline retreat of the entire study reach between August and December 2005. This mode was determined to be

forced by storm surge and wave activity during Hurricane Ophelia and two successive extratropical storms during that period. The second mode, explaining 19% of variance, reflected seasonal cross shore variability of the beach profile with accretion during the summer and fall and erosion during the winter. A cross-shore pivot point between seasonal profiles described by this mode was identified between MSL and MLW for a majority of the transects. Transect 1 fluctuated out of phase with the rest of the transects in this mode indicating potential seasonal flux in along-shore sediment transport which could be related to slight shifts in wave direction or inlet dynamics. This mode strongly correlated to seasonal variability in wave height and energy measured over one to four week averaging windows before each survey. This suggests seasonal forcing of the beach profile by seasonal changes in wave climate. Strong negative correlations were identified in the second mode between increased water levels the day before each survey and landward transport of sediment along transects 2-12. This relationship seems counterintuitive but the strength of correlation indicates significance. Finally, transects 1 and 2 in the vicinity of Lockwood's Folley Inlet exhibited the highest vertical and cross-shore variability within the study area, supporting expansion of the currently defined Inlet Hazard Area (IHA) to the newly proposed IHA which would include transect 2.

ACKNOWLEDGEMENTS

I would like to first thank Dr. William Cleary at the University of North Carolina for providing me a subset of beach profile data from his field work along Oak Island, without which, this research would not have been possible.

I owe special thanks to Dr. Gregg Snedden of the U.S. Geological Survey Wetlands Research Center in Baton Rouge, Louisiana. He provided unending support and guidance in the statistical analysis of beach profile and climate data necessary to conduct this research, and was always willing to take time out of his schedule to answer my questions.

To my advisor, Dr. Lynn Leonard, I thank you for your support throughout my time spent at UNCW in providing me with funding, reviewing this manuscript as well as assisting in preparation of conference presentations. I would also like to thank the rest of my committee, Dr. Jesse McNinch and Dr. Nancy Grindlay for reviewing and providing comments on this manuscript.

DEDICATION

I would like to dedicate this thesis to my wife Cori and my parents Jim and Kathy Baldwin who have provided me with unending support throughout the completion of this research. Cori has stuck by my side as we've tromped up and down the eastern seaboard in my pursuit of a career in coastal research. This is for you Cori.

LIST OF TABLES

LIST OF FIGURES

INTRODUCTION

Coastal change occurs on spatial scales of millimeters to kilometers, and temporal scales of seconds to millennia. For coastal managers, however, the need exists to understand coastal morphology on scales relevant to the decision making process. As a result, over the past several decades, interest has grown in developing methods to study changes in coastal morphology at temporal and spatial scales which allow informed input for management decisions. Communities along the world's coasts are threatened by sea-level rise and subsequent land loss due to inundation and erosion. A combination of thermal expansion of global oceans and melting of glaciers and ice caps has led to a global mean rate of sea-level rise of approximately 3.1 mm/yr since 1993 (IPCC, 2007). As sea-level rises, undeveloped coastal regions naturally retreat landward through processes such as barrier island overwash in which storm waves erode sediment from the front of a barrier and deposit it on the back side of the island (Dolan et al., 1980). Within developed coastal regions, this process is inhibited through beach nourishment, dune development and the construction of hardened barriers – all designed to protect valuable infrastructure. As estimated by the Western Carolina University Program for the Study of Developed Shorelines (WCU-PSDS), nearly two-hundred million dollars have been spent on beach nourishment projects from 1939 to 2006 in North Carolina alone (WCU-PSDS, 2007). In addition to engineered approaches, regulations to restrict development along the oceanfront and in proximity to tidal inlets have been enacted by state and local agencies to help mitigate losses from anticipated coastal erosion. To help coastal communities develop effective strategies to protect their residents while also sustaining the dynamic coastal environment, detailed analyses of shoreline change and the forcing functions that drive this change must be completed on a site-specific basis.

Coastal geologists and engineers interested in patterns of shoreline change have long used topographic beach profile surveys to study how a particular shoreline evolves through time (Winant et al., 1975; Birkemeier, 1984; Larson et al., 1999; Li et al., 2005). Shore-perpendicular beach profile surveys conducted several times a year over several years can provide insight into seasonal and long-term patterns in cross-shore and along-shore sediment movement (Aubrey, 1979; Birkemeier, 1984). Topographic profiling methodology has evolved over time as new technologies have emerged. Currently, many beach profile surveys are conducted using real-time kinematic global positioning systems (RTK GPS) which provide vertical and horizontal accuracy to within a few centimeters. After a multi-year set of beach profiles has been collected, the data must be properly analyzed to yield meaningful results. Typically, this process involves determination of change along individual, repeatedly surveyed transects over time. While this type of analysis can reveal transect specific patterns, a study involving a large number of transects over a long period of time can become cumbersome.

Originally developed for meteorological applications, empirical orthogonal function (EOF) analysis (Pfiesendorfer, 1988) has been embraced by coastal geologists and engineers as a useful analytical tool for identifying spatial and temporal patterns of beach and nearshore topographic variability from large data sets (Winant et al., 1975; Birkemeier, 1984; Wijnberg and Terwindt, 1995; Larson et al., 1999; Haxel and Holman, 2004). EOF analysis identifies patterns of variability in a matrix of time series data collected through space. Each of these patterns (also called “modes”) has a unique spatial and temporal signature and explains a specific percentage of the total variability in the time series. Birkemeier (1984) used EOF analysis of beach and nearshore profiles to identify storm response of sand bar configurations in Duck, North Carolina. At Torrey Pines Beach in California, Winant et al. (1975) conducted an EOF analysis on similar data and identified seasonal cross-shore sediment exchanges between the bar and berm as the dominant pattern of variability. Haxel and Holman (2004) identified seasonal accretion and erosion of a dune field due to changes in wind patterns as the dominant pattern of variability at Agate Beach, Oregon. These and other studies have shown that modes of variability resulting from an EOF analysis can frequently be linked to specific forcing functions. Establishing this linkage is important, as output from the EOF analysis simply partitions statistical variability without identifying physical processes. Through the use of EOF analysis and the study of local forcing functions, one can identify the most significant patterns of variability in a dataset and, potentially, the processes driving that variability. Identification of these patterns and processes in the coastal environment is essential to developing effective coastal management strategies.

This study examines variability in beach topography as well as the local wave, water level, and wind conditions from June 2004 to June 2006 along Long and Yaupon beaches on Oak Island, North Carolina. The objective of this study is to utilize EOF analysis to identify spatial and temporal patterns of variability in beach topography during the proposed study period, and to explore linkages between topographic variability and forcing by local wave, water level and wind conditions.

STUDY AREA

This study was conducted along the central and western coast of Oak Island, North Carolina. Oak Island is a 21.5 km-long, south-facing Atlantic barrier beach located on the western arm of the Cape Fear Foreland in southeastern North Carolina (Figure 1). The North Carolina barrier island system is largely influenced by its underlying geology, and therefore can be split into two main regions. To the north of Cape Lookout, long thin barriers are underlain by thick Quaternary-aged unconsolidated sediments which extend to a depth of up to 70 meters in the vicinity of the Albermarle Embayment (Cleary, 2000). South of Cape Lookout, the barrier system is composed of shorter barriers with a thin veneer of Quaternary sediments underlain by Upper Cretaceous to Miocene age rocks (Cleary, 2000). These rocks frequently outcrop within the shoreface where Quaternary sediments are particularly thin. Oak Island lies within this southern region of North Carolina barriers. In both regions, the underlying geology is cut by paleo-fluvial channels which filled with unconsolidated sediment as sea-level rose and valleys flooded during the Holocene transgression. Between these in-filled paleo-fluvial channels lie interfluvial headlands typically composed of more consolidated material. This complex paleo-topography has led to classification of coastal regions throughout the North Carolina barriers as headland or non-headland dominated based on underlying geology (Riggs et al., 1995).

Oak Island is composed of three main geologic segments including a central Pleistocene headland flanked by two non-headland transgressive spits (Figure 1). Yaupon Beach is a 3.5 km-long, subaerial, Pleistocene headland composed predominantly of humate sandstone and coquina limestone (Cleary et al., 2000). To the west of Yaupon Beach lies Long Beach, a 14 km–long transgressive spit. To the east is Caswell Beach, a 4 km-long transgressive spit (Cleary et al., 2000). The island is flanked by Lockwood's Folley Inlet to the west which connects to the Atlantic Intracoastal

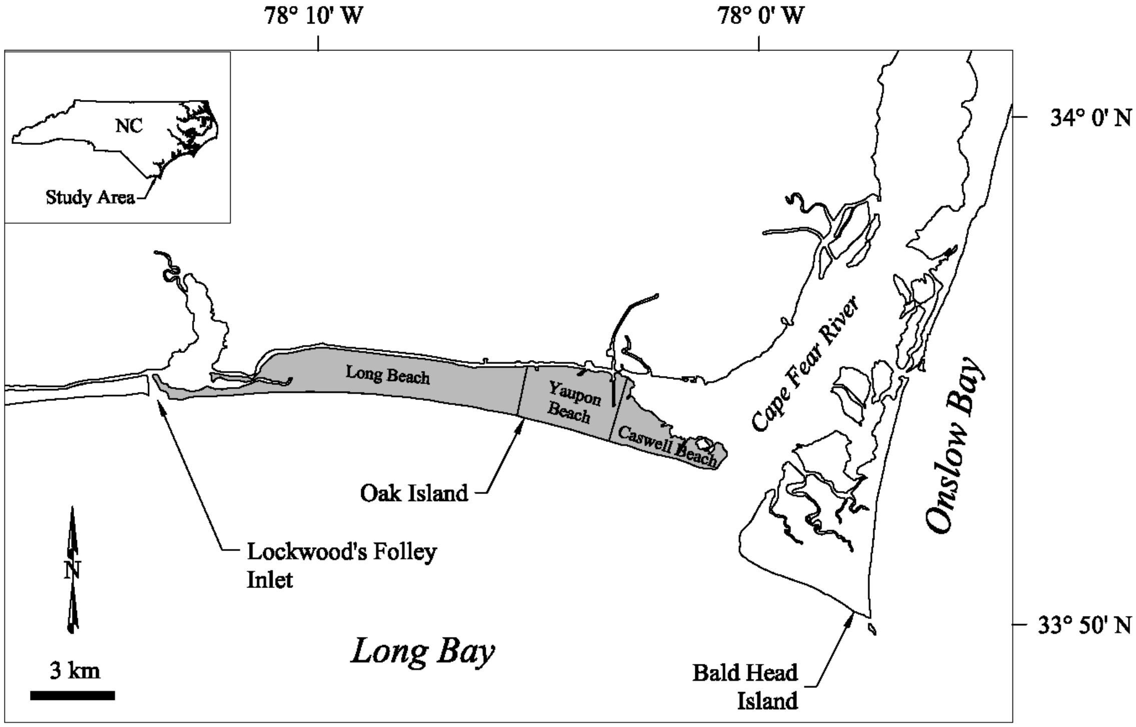

Figure 1. Location of study area and geologic segments – Oak Island, North Carolina. Yaupon Beach is a Pliestocene subaerial headland surrounded by two transgressive spits including Long Beach to the west and Caswell Beach to the east.

Waterway (AIW), and the mouth of the Cape Fear River to the east (Figure 1). The AIW separates Oak Island from the mainland.

Oak Island lies within Long Bay which extends from Cape Fear southwest to Cape Romain in South Carolina. Long Bay has a mean annual significant wave height of 0.6 m, a dominant wave period of 6.5 s, and a mean tidal range of 1.3 m (Davis, 2006). Tucked behind the wave shadow of Cape Fear, Long Bay is a relatively low energy environment. In comparison, Onslow Bay, which lies to the north between Cape Fear and Cape Lookout, has a mean annual significant wave height of 1.5 m, a dominant wave period of 8.0 s and a mean tidal range of 1.0 m (Wren, 2005). Although Long Bay is a relatively low energy environment, the passing of tropical storms and hurricanes through the Cape Fear region has caused severe erosion events along Oak Island due to associated storm surge and wave activity. The late 1990s were particularly active with six hurricanes passing through or making landfall in the Cape Fear region, including Hurricane Floyd, which brought a 2-m surge that eliminated most of the artificial dune system along the island and caused extensive property damage. Large scale infrastructure damage and beach erosion from this storm lead to two major beach nourishment projects along Oak Island.

In 2001, in an effort to replenish the eroded beach and restore sea turtle nesting habitat, the U.S. Army Corps of Engineers (USACE) placed approximately 2.03 million m^3 of sediment along 3.8 km of the central Oak Island coast (Figure 2). Soon after completion, a separate project conducted by the USACE placed additional sediment along Oak Island obtained from the Wilmington Harbor Deepening Project. By April of 2002, approximately 1.91 million m^3 of suitable dredged material had been placed along

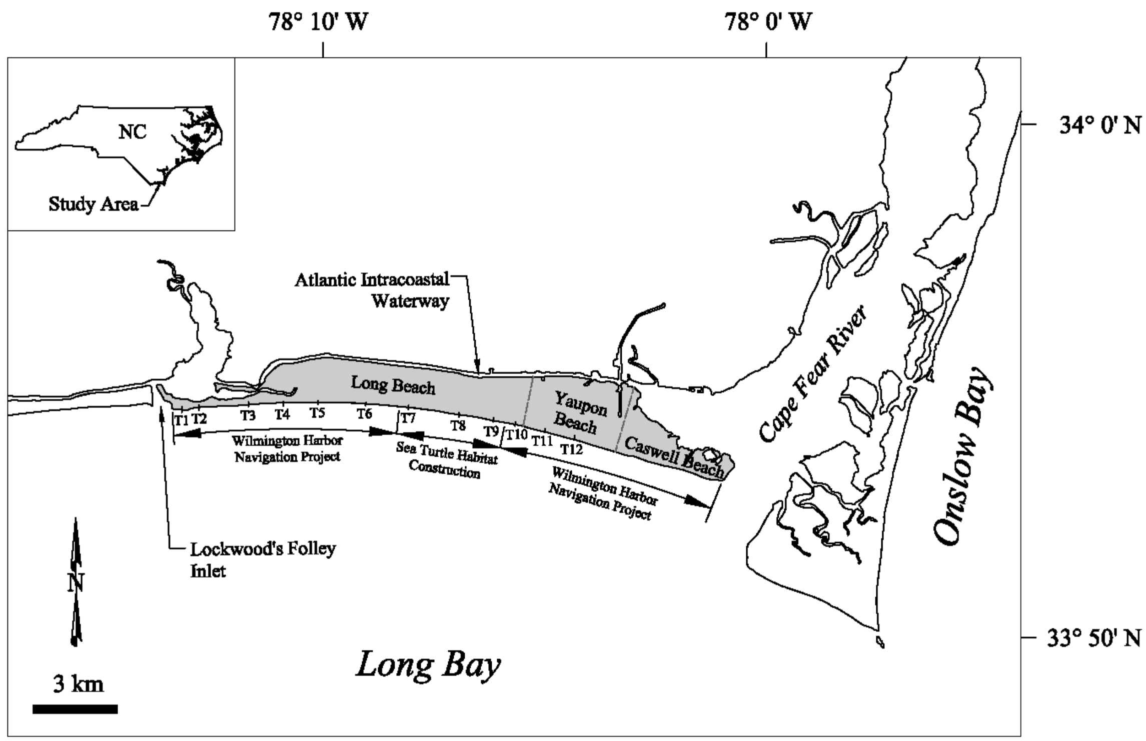

Figure 2. Location of recent beach nourishment projects along Oak Island and beach profile transects (T1-T12). The Sea Turtle Habitat Construction Project was completed in May 2001 and included placement of approximately 2.65 M cubic yards (cy) of sand along 3.8 km in eastern Long Beach. The remainder of the island was nourished with approximately 2.5 M cy of sand dredged during the Wilmington Harbor Navigation Project by April 2002.

the remainder of Oak Island (Figure 2). Together, sand placement from these two projects led to a much needed increase in beach width along the entire oceanfront shoreline of Oak Island.

METHODS

Beach Topography Data Collection

Beach topography data were aggregated from bimonthly beach profile surveys collected along Oak Island from 1997 to present by Dr. William Cleary of the University of North Carolina Wilmington. These data include shore-perpendicular transects spaced at along-shore distances varying from 0.5 km to nearly 2 km within the study area (Figure 2). During surveys, horizontal and vertical measurements are made at 1-m intervals along each transect from landward of the primary dune to wading depth, which typically coincides with Mean Lower Low Water (MLLW). Prior to 2004, these surveys were conducted with rod and level techniques. Since 2004, these surveys have been conducted with RTK GPS. Horizontal measurements are referenced to the 1983 North American Datum (NAD83) – North Carolina State Plane coordinate system. Vertical measurements are referenced to the 1988 North American Vertical Datum (NAVD88).

Only data collected bimonthly from June 2004 to June 2006 were available for this study. These data were collected with RTK GPS, thereby maximizing horizontal and vertical accuracy of the measurements. A total of 13 surveys were available for analysis from this time period. A two-year study period was sufficient in duration to allow for the identification of seasonal and/or annual patterns in shoreline change within the study area. The temporal spacing of these surveys, however, meant variability occurring at shorter time scales were not identified. In addition, beginning the study in June 2004 allowed two years for equilibration of the renourished beach which was completed in April 2002.

EOF Analysis of Beach Topography Data

To identify spatial and temporal patterns of variability in beach topography within the study area, EOF analysis was used to analyze the 13 surveys conducted for each of 12 transects along Long and Yaupon beaches. The utility of EOF analysis lies in its ability to take a time series of data and convey a majority of the variability in the dataset in fewer, uncorrelated time series, referred to as "modes". Each of these modes has a unique spatial and temporal pattern and explains a specific percent of variance in the time series studied.

In this study, input data for the EOF analysis consists of an M x N matrix of beach surface elevations (matrix X; Figure 3) collected at M locations within the study area N different times. The analysis requires a matrix of elevation values measured at the same horizontal location along each transect throughout separate surveys. Elevation values were measured at one meter intervals along predetermined transects in the field using a GPS. Since exact replication of each transect could not be accomplished in the field (Figure 4a), standardization of these points was required. Standard grid nodes were placed along each of the 12 transects at three meter intervals (Figure 4b). Field-measured elevations from each survey period were then gridded to these standard nodes using nearest neighbor interpolation in MATLAB. An $M \times N$ matrix was then created for each transect (Figure 4c) out of the standardized elevation values from each survey date. Periodic gaps in the matrices occurred along the seaward portions of transects when wading depths were exceeded due to cross-shore variations in beach width (Figure 4c).

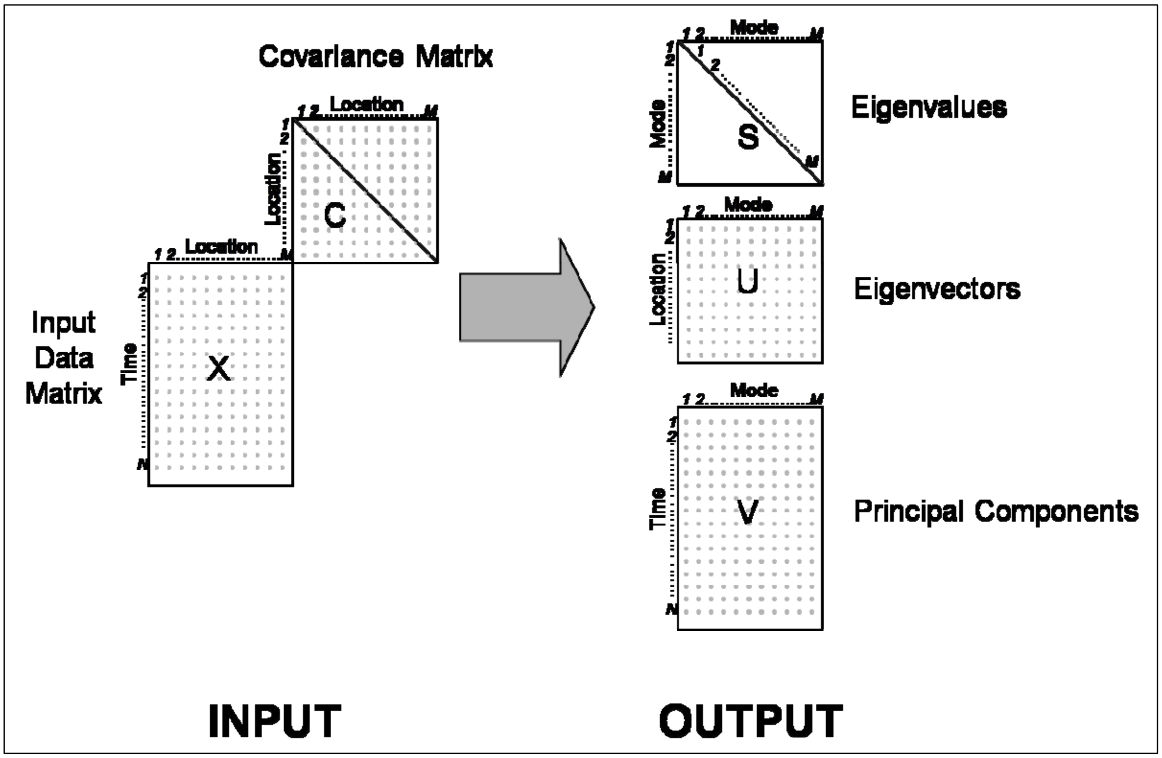

Figure 3. Diagram showing format of input and output data for an Empirical Orthogonal Function analysis.

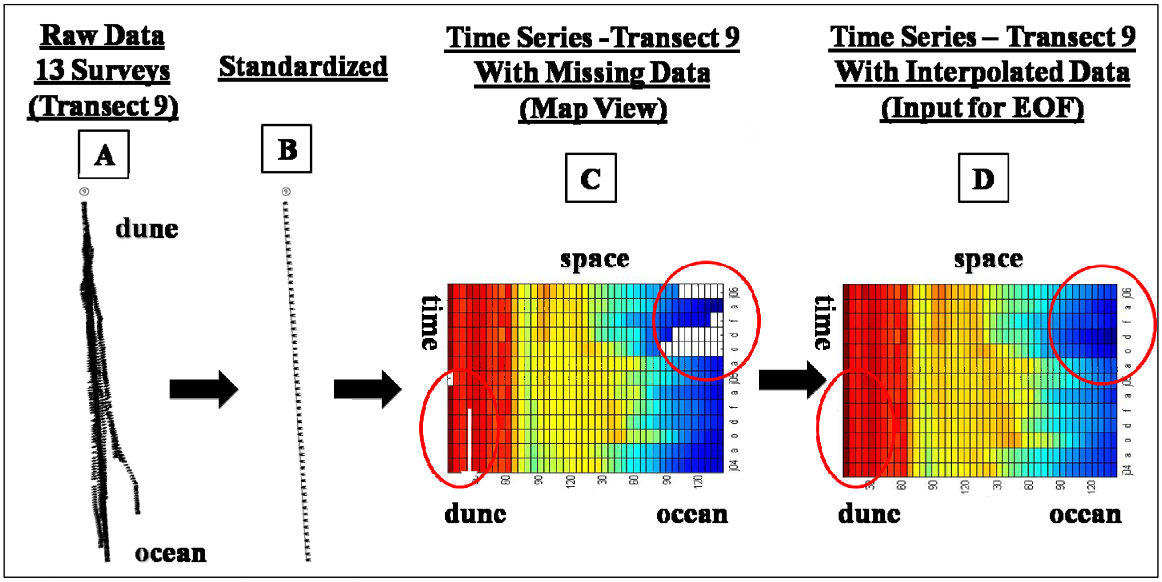

Figure 4. Example of the steps required to create an input matrix for the EOF analysis. A) Map view of raw xyz data collected every meter along the transect. B) Raw data was then projected to standardized nodes placed at three meter intervals along the transect. C) A time series of standardized elevations was then created for the 13 surveys of the transect. D) Finally, missing data was filled in using a combination of extrapolation and interpolation.

There also were occasional gaps in the landward portions of transects, but these missing data were far less frequent. Missing data at the seaward end of each transect were extrapolated using the slope of the last two measured points on the transect. Because little variability occurred in the most landward portions of the transects, and extrapolation through space beyond the crest of the dune could have created unrealistic dune heights, missing data at the landward end of each transect were linearly interpolated through time. Transect 10 (Figure 2) was not measured during the October 2005 survey due to loss of instrument power. This entire transect was interpolated through time as described above. Table 1 details missing data in the time series matrix for each transect as well as information on where missing data were located. After extrapolation and interpolation of missing values, all transect time series were combined and vectorized to run the EOF analysis on transects 1-12 simultaneously. Vectorization of all transects into one time series allows the analysis to identify both cross-shore and along-shore variability across the entire study area. Early researchers conducting EOF analyses on beach profile data concluded that the first mode identified in the analysis represented the mean beach elevation throughout the study period (Winant et al., 1975). Subsequent modes thus represent patterns of variability beyond the mean beach elevation. Since this variability is the primary concern of this study, the vectorized matrix was de-meaned before conducting the EOF analysis to ensure results of the analysis identified patterns of variability beyond the mean beach elevation.

The EOF analysis was then performed on the covariance matrix of the input data series (matrix C; Figure 3) in MATLAB. The analysis produces a number of modes of variability equal to the number of locations measured (M) in the input data matrix, with

Transect ID	Transect Length (m)	Size of Matrix (nodes x time)	Landward Missing	Seaward Missing	Total Missing	Total # of Cells	% Missing
1	162	55 x 13	4	54	58	715	8.1
2	129	44 x 13	1	31	32	572	5.6
3	99	34 x 13	3	23	26	442	5.9
4	114	39 x 13	4	61	65	507	12.8
5	99	34 x 13	3	39	42	442	9.5
6	99	34 x 13	11	30	41	442	9.3
7	129	44 x 13	0	31	31	572	5.4
8	138	47 x 13	14	24	38	611	6.2
9	132	45 x 13	13	23	36	585	6.2
10	108	37 x 13	22	29	51	481	10.6
11	105	36 x 13	3	15	18	468	3.8
12	96	33 x 13	7	18	25	429	5.8
			TOTALS				
			85	**378**	**463**	**6266**	**7.4**

Table 1. Missing beach profile data requiring interpolation. A total of 7.4% of data included in the input matrices for the EOF analysis were missing. Missing data on the seaward end of transects were extrapolated through space using the slope of the last two measured points on the transect. Missing data on the landward end of transects were interpolated through time. Of the 7.4% of missing data, 18% were missing from the landward portion of the transects and 82% were missing from the seaward portions.

the modes arranged from greatest to least importance. The top few modes typically explain a large proportion of the total dataset variability while the remaining modes represent noise in the data (Winant et al., 1975). Each mode consists of three components: an eigenvector, a principal component (PC), and an eigenvalue. The eigenvector (matrix *U*; Figure 3) describes the spatial pattern of variability of the mode. Each mode is associated with a time series (or principal component; PC; matrix *V*; Figure 3) that describes the eigenvector's evolution through time. Finally, the eigenvalue (diagonal elements of matrix *S*; Figure 3) identifies the percentage of the total variability that each mode describes. Results of the EOF analysis were normalized to their standard deviations, giving principal components a non-dimensional variance of unity, and causing eigenvectors to carry units of meters, as measured in the original survey data. Since the input matrix was de-meaned before the analysis, the mean beach surface was added back into the resulting eigenvectors. This allows a better spatial representation of each mode as variability superimposed on the mean beach profile.

Wave Climate and Water Level Analysis

Wave data were collected from three wave observation stations in Long Bay in close proximity to the study area on Oak Island (Figure 5). The USACE maintains two of these stations (OKI and BHI), and data from each station is available on the USACE Field Research Facility's website (usace.frf.army.mil). Each station consists of a bottom mounted acoustic doppler current profiler (ADCP) measuring both speed and direction of currents within the water column as well as wave characteristics above the instrument. Station OKI is located 2.2 kilometers south of Oak Island, and station BHI is located 1.6 kilometers south of Bald Head Island (Figure 5). The third station is operated by the

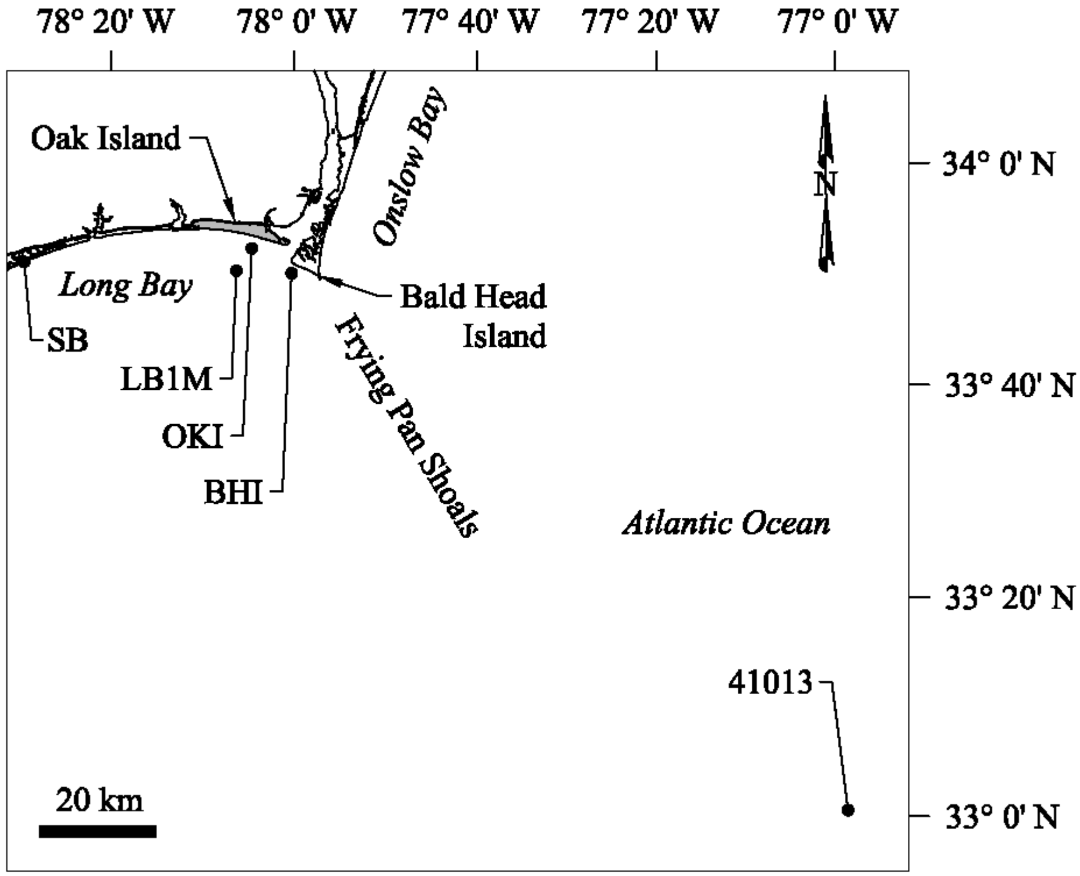

Figure 5. Location of wave, wind, and water-level observation stations used to characterize local conditions. Stations OKI, BHI and LB1M were used to compile wave data. Stations OKI and BHI are ADCPs operated by the United States Corps of Engineers. Station LB1M is an ADCP operated by the UNCW Coastal Ocean Research and Monitoring Program. Station 41013 is a buoy operated by NOAA from which wind data were collected. Water-level data were collected from a NOAA tide gauge at Sunset Beach (SB).

UNCW Coastal Ocean Research and Monitoring Program (CORMP), and raw data is available from their website (www.cormp.org). This station, LB1M, is also a bottom-mounted ADCP and is located 6.5 kilometers south of Oak Island (Figure 5). Station OKI recorded hourly measures of significant wave height (*Hs*), dominant wave period (*Tp*), propagation direction of the dominant wave period (*Dp*), and water depth. Station BHI and LB1M both recorded the same wave parameters, however BHI recorded at three hour intervals. LB1M recorded at two hour intervals from November to December of 2004, and then at four hour intervals through June of 2006.

Unfortunately, none of these stations produced a complete time series of measurements for the study period, nor did they sample over identical time intervals. Because OKI was closest to the study area and provided the most complete time series, it was selected as the station to be used to conduct the wave climate analysis. To form a single, more complete, time series of wave data, linear regressions were used to quantify relationships between wave parameters at OKI, BHI, and LB1M, and those relationships were used to predict missing values in the OKI record.

Before OKI wave parameters could be predicted from BHI and LB1M, all records were linearly interpolated to an hourly sampling interval. Gaps greater than 12 h were not interpolated, and thus were left as missing data. Missing significant wave height data from OKI was predicted by applying regression equations to data collected from both BHI and LB1M. A 72-hour low pass filter was first conducted on *Hs* data at all three stations to reduce the influence of wave chop and gain stronger correlation coefficients during regressions (Figure 6). Using these prediction formulas, gaps in *Hs* at OKI were first filled in with predictions from BHI, and then with predictions from LB1M. For *Tp*,

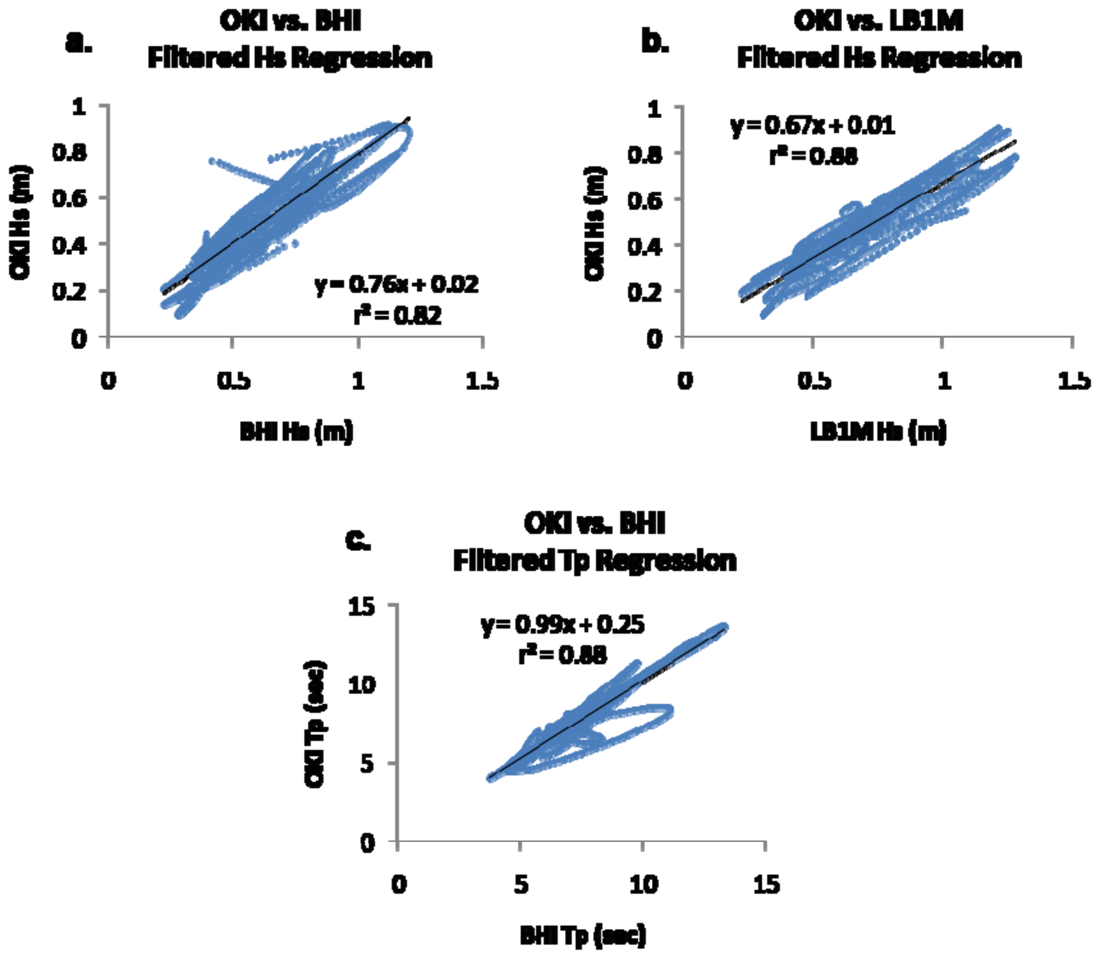

Figure 6. Results of regressions between wave data stations used to create wave record. Regressions shown are for Hs between stations OKI and BHI (a), OKI and LB1M (b), and for Tp between stations OKI and LB1M (c).

a 72-hour low pass filter was applied to paired OKI and BHI measurements and a regression equation was used to fill in missing data at OKI from BHI. A simple regression of paired directions between stations would not work because wave direction is a vector quantity. To fill in the gaps in directional data at OKI using data from BHI, vector correlation (Crosby et al. 1993) was conducted between paired directional data for the two stations. Wave directions for each station were first split into their easting (u) and northing (v) components. A 72-hour low pass filter was then applied to all u and v components to remove short-period fluctuations in wave direction. Finally, a vector correlation was completed between paired u and v components for each station. Unlike simple regressions, the correlation coefficient resulting from this method ranges between zero and two. Zero indicates no correlation and two indicates perfect correlation (Crosby et al., 1993). Coefficients greater than 0.6 are considered relatively high, and indicate linear dependence between time series (Crosby et al., 1993). The resulting coefficient for the vector correlation between filtered u and v components at OKI and BHI was 1.2. The prediction formula was:

$$\text{OKI Dir} = \text{BH Dir} + 6.8°$$

indicating that wave direction at OKI was generally 6.8 degrees clockwise to wave direction recorded simultaneously at BHI. Subsequent interpolation of the data resulted in a more complete wave record for station OKI, however, gaps in the record remained where measurements were missing for all three stations. Once the more complete wave record was compiled, a number of other wave parameters were calculated from the data including wave length (*L*), steepness, and energy (*E*) (Figure 7). Monthly means for

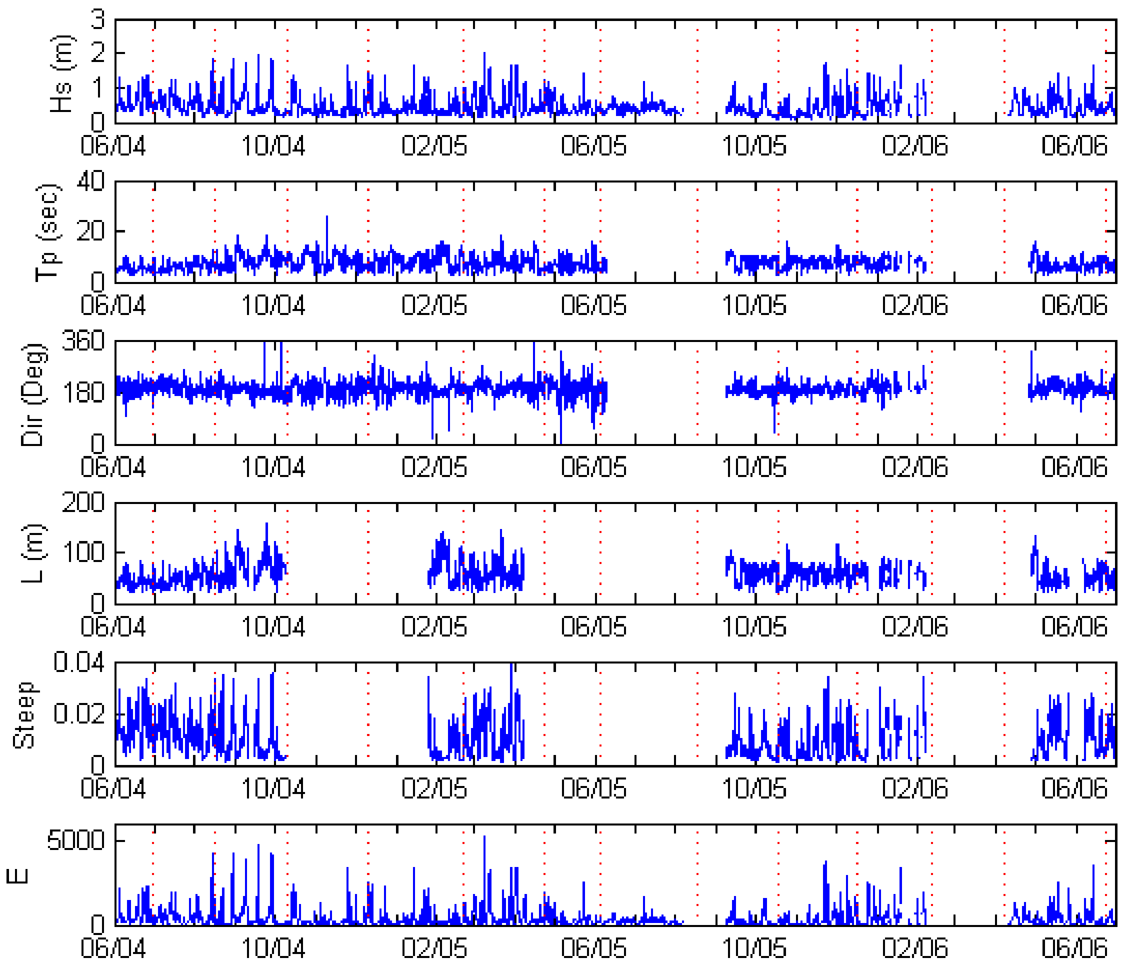

Figure 7. Station OKI wave record including data extrapolated from stations BHI and LB1M. Vertical red lines represent dates of beach profile surveys conducted during the study period.

wave height, period, direction, wave length, steepness, and energy were calculated to identify any seasonality or trends in the wave record during the study period.

Water level data were collected every 6 minutes from NOAA tide gauge 8659897 located off of the Sunset Beach fishing pier, approximately 26 km west of the study site (http://tidesandcurrents.noaa.gov/index.shtml; Figure 5). These data were converted from a vertical reference datum of Mean Lower Low Water (MLLW) to NAVD88 to match the datum in which the topography data was collected. Surge for specific storm events and residual sea level throughout the study period was calculated by subtracting the predicted from observed water levels at Sunset Beach.

To determine whether patterns of variability in local wave and water level data could be related to patterns of variability in beach topography, correlations were conducted between principal components identified in the EOF analysis and each of the wave and water level parameters identified above. Because the beach profile, wave, and water level data were collected at different temporal scales (bimonthly for beach profile surveys, every three hours for wave data, and every six minutes for water level data), the data sets were first converted to comparable temporal scales using a methodology similar to Miller and Dean (2007). For this study, both mean and maximum (except for wave direction) values were calculated for each of the wave and water level parameters over time periods including one day, one week, and one month before each beach profile survey as well as the entire period between surveys (approximately bimonthly). Only mean values were calculated for wave direction. Reduction of wave and water level data to mean and maximum values over these time scales was necessary to reduce the wave record to the size of the principal component time series which include 13 values (one for each beach profile survey included in the analysis). Reduction of these data also allowed this study to test whether ambient wave conditions over shorter or longer time periods are more important in driving the patterns of variability identified in the EOF analysis. Correlations with p-values less than 0.05 were significant.

Wind Climate Analysis

Wind data were gathered from the National Oceanic and Atmospheric Administration (NOAA) National Data Buoy Center (NDBC) Station 41013, located on Frying Pan Shoals approximately 65 km southeast of Oak Island (Figure 5). Station 41013 consists of a three-meter discus buoy with an anemometer mounted five meters above the sea surface. Wind measurements made at this station include wind speed and wind direction, which are averaged and reported over ten minute periods. These data were reduced to measurements taken every three hours by sub-sampling to match the data collection interval for wave data. Gaps in wind data also occurred at this station due to instrument malfunction; however, these missing data were not interpolated due to the lack of sufficient alternate wind data in the near vicinity. Monthly means for wind speed and direction, and monthly maximums for wind speed were calculated to identify any seasonality and or trends in the wind record during the study period. A wind rose was also created from the available data using WRPLOT View© to identify dominant wind directions and magnitudes during the study. Finally, mean wind speed, maximum wind speed, and mean wind direction were calculated for the day, week, and month (30 days) before each beach profile survey as well as the entire period between surveys (approximately 60 days). These values were then correlated against the principal component time series for the EOF modes to determine whether significant relationships exist ($p<0.05$) and whether wind conditions over shorter or longer time scales were more closely related to patterns of variability in beach topography identified by the EOF analysis.

RESULTS

EOF Analysis

Results of the EOF analysis show that the first two modes alone account for 63% of variability in beach topography data (44% and 19% respectively) (Figure 8). These percentages are obtained from the eigenvalues. Because these two modes explain the majority of variability in the data, this study focuses on analysis and interpretation of these two modes only.

Mode 1 (M1)

M1 represents 44% of observed variability in beach topography along Long and Yaupon beaches during the two-year study period. The M1 eigenvector describes the spatial pattern of variability exhibited by this mode (Figure 9a). Regions with positive eigenvector values fluctuate out of phase with regions of negative eigenvector values. The seaward portions of each of the 12 transects contain values between zero and one indicating these regions vary in-phase with each other over time, although each transect fluctuates with different magnitudes. The highest variability exhibited by this mode occurs along the seaward portions of transects 1, 2, and 8 shown in hot colors on Figure 11a. The M1 PC explains the temporal pattern of variability for this mode (Figure 9b). From June 2004 to August 2005, PC values are positive, fluctuating only slightly.

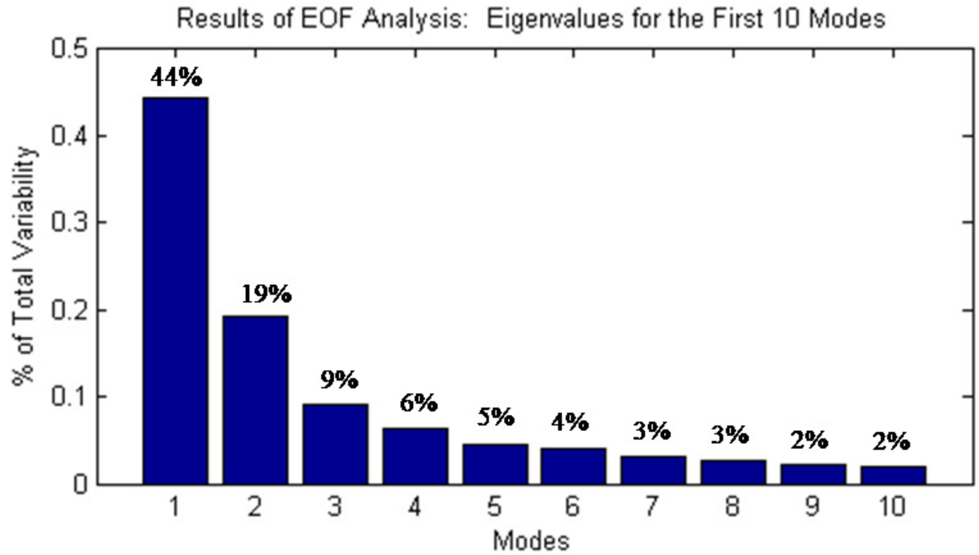

Figure 8. Eigenvalues for the first ten modes of the EOF analysis. These values represent the percentage of total observed variability each mode explains. Combined, the first ten modes represent 98% of total variability with modes 1 and 2 accounting for the majority of variability in the data set (63%).

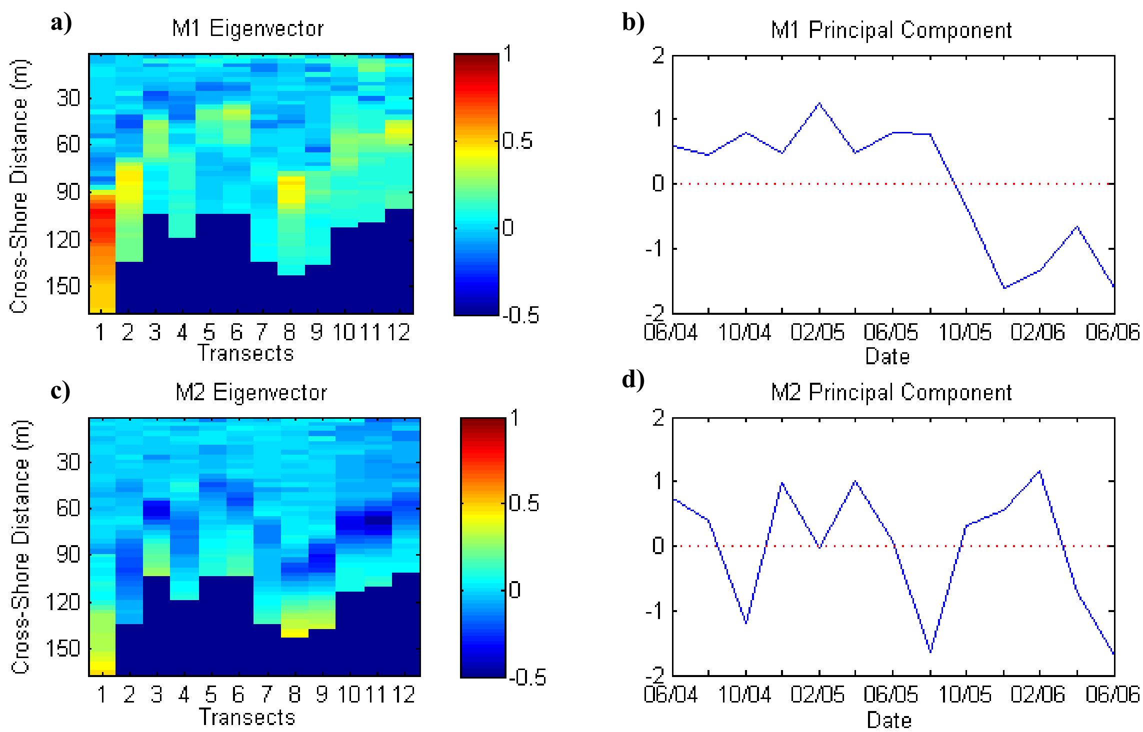

Figure 9. Eigenvectors and principal components for first two modes of EOF analysis. Eigenvectors are graphed as a map view with colors representing variability in elevation. a) M1 (44%) Eigenvector, b) M1 PC, c) M2 (19%) Eigenvector, d) M2 PC.

Between August 2005 and December 2005, PC values shift sharply negative, and then remain negative through June 2006 with a slight positive fluctuation in April.

Multiplication of the M1 eigenvector by each of the 13 PC values allows inspection of how the spatial pattern of variability described by this mode evolves through time. The M1 PC indicates this mode explains a large shift in beach configuration between August and December 2005 with relative stability before and after this period. Therefore, the M1 eigenvector was multiplied by the August and December 2005 PC values to study the change in beach configuration during this time, as described by this mode (Figure 11b and Figure 11c). In addition, the location of MHW (+0.55 m NAVD 88) was plotted on each figure as a reference. Figure 11b shows higher beach surface elevations and a more seaward position of MHW in August 2005. Since the PC values before this survey were all positive, this mode suggests a similar beach configuration from the June 2004 to August 2005. From August to December 2005, beach surface elevations decrease rapidly and MHW retreats landward (Figure 11c). The most severe erosion exhibited by M1 during this period occurred at transects 1, 2, and 8 with landward retreat of MHW on the order of 32 m, 14 m, and 13 m respectively. After December 2005, beach surface elevations remained low through the end of the study period, as indicated by negative PC values, with only slight accretion in April 2006.

Locations exhibiting high vertical variability as described by M1 were identified by calculating the difference in M1 beach surface elevations between August and December 2005 PC values (Figure 11). Elevation change between August 2005 and December 2005 was greatest at the seaward portion of transect 1 where the beach

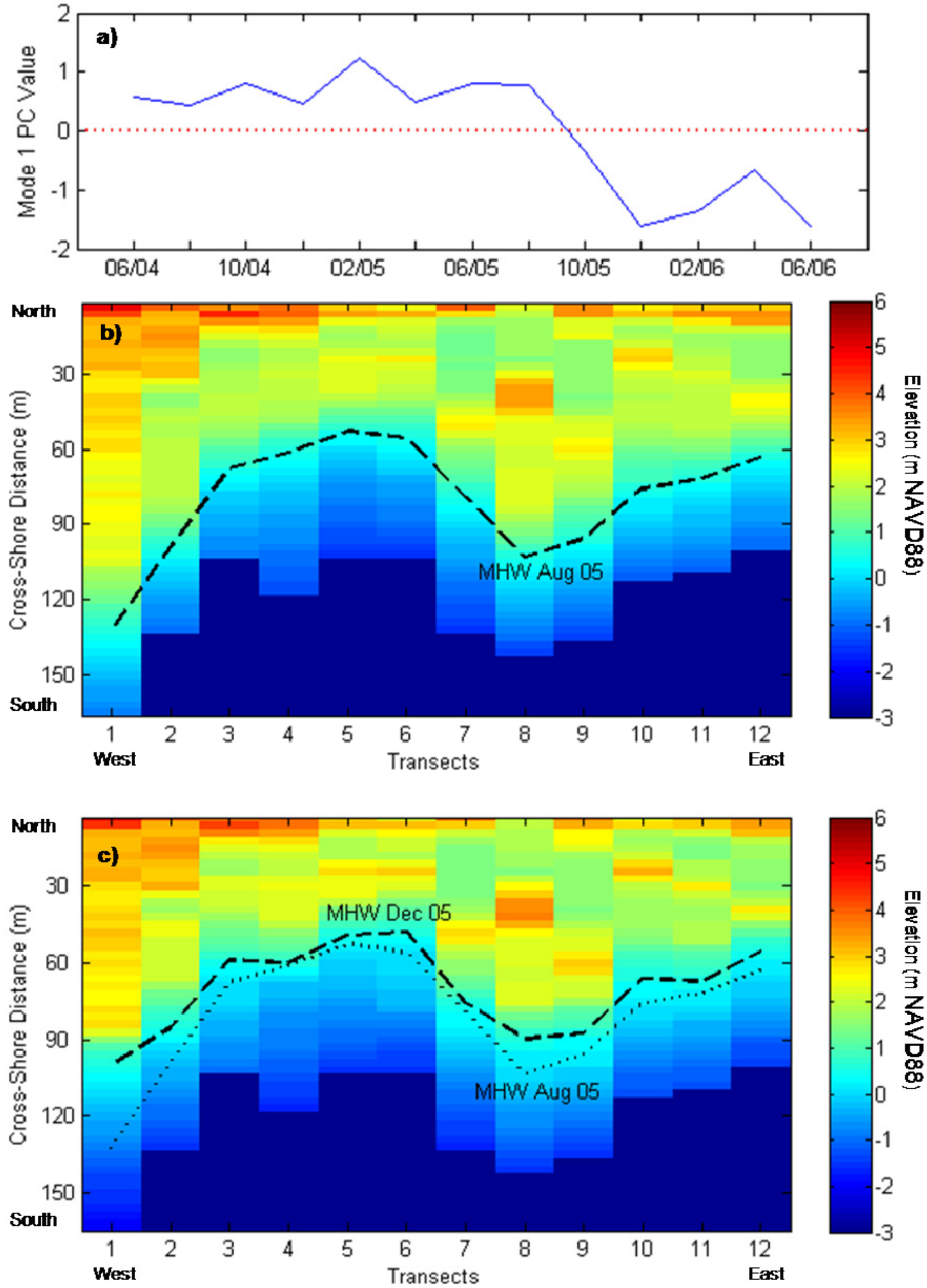

Figure 11. Fluctuations in beach topography exhibited by M1 between August and December 2005. a) M1 PC. b) Map view M1 beach configuration at August 2005 PC value. c) Map view M1 beach configuration at December 2005 PC value. MHW = +0.55 m NAVD88.

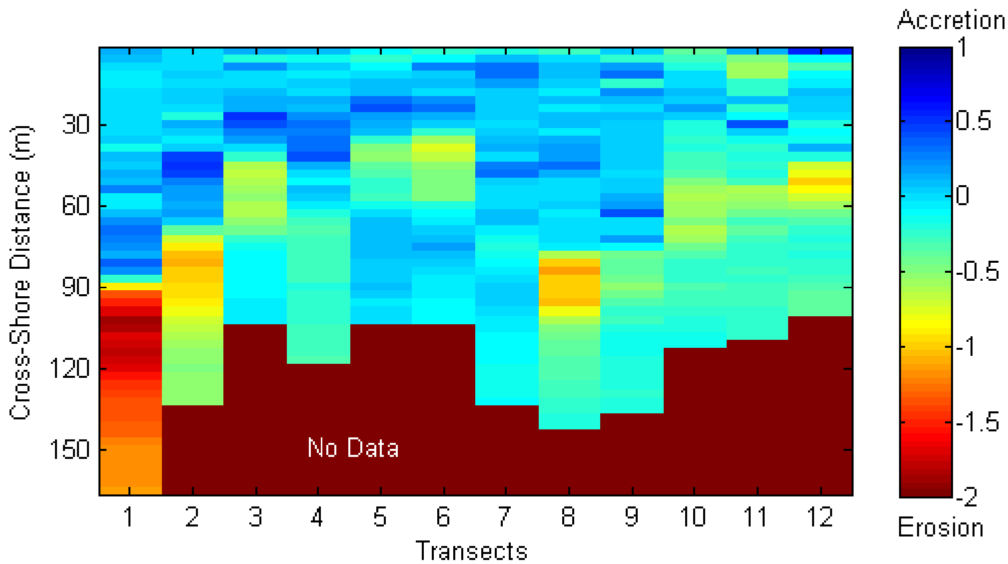

Figure 11. M1 vertical changes in elevation between the August and December 2005. Negative values represent vertical erosion in meters from August to December and positive values represent vertical accretion.

vertically eroded as much as 1.9 m. The seaward portion of the remaining transects lost between 0 and 1.3 m vertically during the same time period.

The pre-interpolation surveyed beach profiles at transects 1, 2, and 8 were plotted for the August, October, and December 2005 surveys (Figure 12) to compare to M1 results from the EOF analysis. These surveyed profiles show that at transect 1, MHW retreated landward 10.9 m from August to October and 19.7 m from October to December for a total of 30.6 m. The highest surveyed vertical change in elevation at transect 1 was consistent with M1, and showed a loss of 2.1 m approximately 100 m seaward of the landward end of the transect. At transect 2, surveyed MHW moved landward 12.5 m from August to October, and seaward 0.8 m from October to December for a total landward movement of 11.7 m. The largest surveyed loss in elevation at transect 2 was 1.2 m and occurred approximately 90 m seaward of the landward end of the transect. Similar to transect 2, surveyed MHW at transect 8 moved 16.3 m landward from August to October and 2.2 m seaward from October to December for a total landward movement of 14.1 m. Figure 13 and Table 2 show the surveyed cross-shore movement of MHW between August and December 2005 for all 12 transects. Across the study area, surveyed MHW retreated landward a mean 8.9 m between August and October and landward again 2.9 m between October and December for a total mean shoreline retreat of 11.8 m. These results indicate that a majority of erosion described by this mode occurred between August and December 2005.

Mode 2 (M2)

M2 accounts for 19% of the total variability in beach topography along Long and Yaupon beaches during the study period (Figure 8). The eigenvector and PC for this

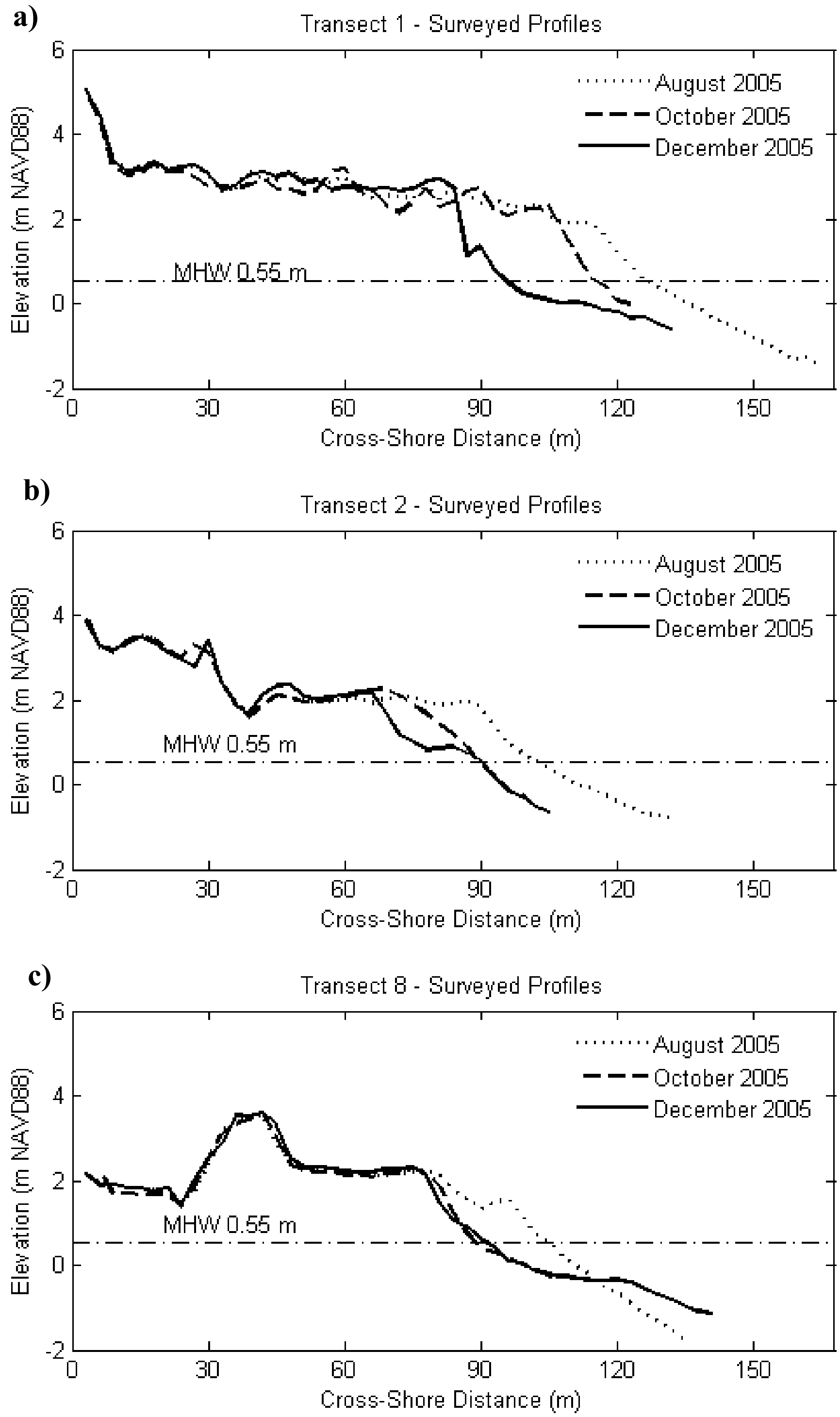

Figure 12. Surveyed profiles for transects 1(a), 2(b), and 8(c) during August, October, and December 2005.

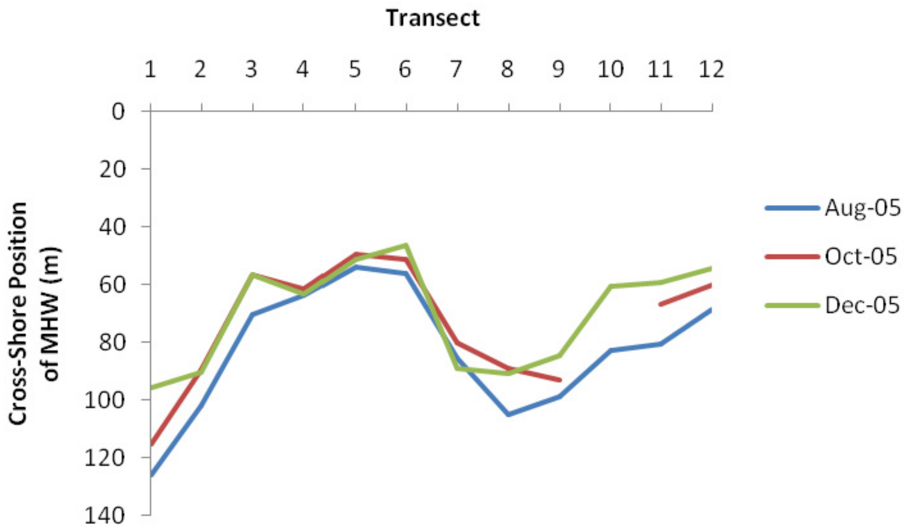

Figure 13. Surveyed cross-shore position of MHW during August, October and December 2005 beach profile surveys. Transect 10 was not surveyed during October 2005 survey due to loss of instrument power.

Transect	Aug05 - Oct 05	Oct05 - Dec05	Aug05 - Dec05
1	-10.9	-19.7	-30.6
2	-12.5	0.7	-11.8
3	-13.8	-0.2	-14.0
4	-2.3	1.6	-0.6
5	-4.3	1.7	-2.6
6	-4.6	-5.2	-9.8
7	-5.3	8.9	3.6
8	-16.3	2.2	-14.1
9	-5.4	-8.4	-13.9
10	NA	NA	-22.0
11	-14.0	-7.6	-21.5
12	-8.5	-5.8	-14.3
Mean	**-8.9**	**-2.9**	**-11.8**

Table 2. Surveyed cross-shore movement of MHW between August, October, and December 2005 beach profile surveys. Transect 10 was not surveyed during October 2005 due to loss of instrument power.

mode are shown in Figure 9c and Figure 9d respectively. While the M1 PC shows a single, large shift in beach configuration during the study period, the M2 PC exhibits a more cyclical pattern (Figure 9d). Apart from the June and August 2004 values, the M2 PC shows peak positive values in the winter and early spring, and peak negative values in the summer and early fall. To assess the presence of an annual period in the data, a harmonic regression (Emery and Thomson, 1997) with a period of 12 months was conducted on the M2 PC. This resulted in an r^2 value of 0.36 (Figure 14) indicating this mode does exhibit annual periodicity with fluctuations in beach topography between summer and winter configurations (minimum and maximum PC values).

The spatial pattern of variability exhibited by this mode was inspected by multiplying the M2 eigenvector by the maximum PC value which occurred in February 2006 (Figure 15b), and by the minimum PC value, which occurred in June 2006 (Figure 15c). This gives the two end member, seasonal configurations of beach topography described by this mode, between which, fluctuations occur throughout the study period. The spatial pattern of variability for this mode is unlike M1 in that not all transects fluctuate in-phase with each other. In M2, transects 2-12 fluctuate in-phase with each other but out-of-phase with transect 1. This pattern is exhibited when MHW is plotted on the February and June 2006 M2 beach configurations (Figure 15c). From February to June 2006, M2 shows MHW retreating landward 10.3 m at transect 1 and advancing seaward an average of 9.1 m at transects 2-12. So for M2, positive PC values, occurring predominantly in the winter, represent a landward retreat of the shoreline at transects 2-12 and a seaward advance at transect 1. Inversely, negative M2 PC values, occurring

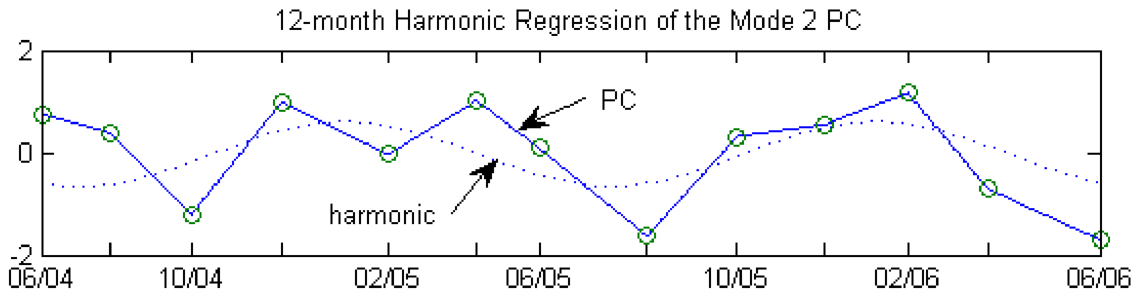

Figure 14. Harmonic regression of the M2 PC with an annual period of 12 months. The r^2 value for this regression is 0.36 showing this PC exhibits annual periodicity.

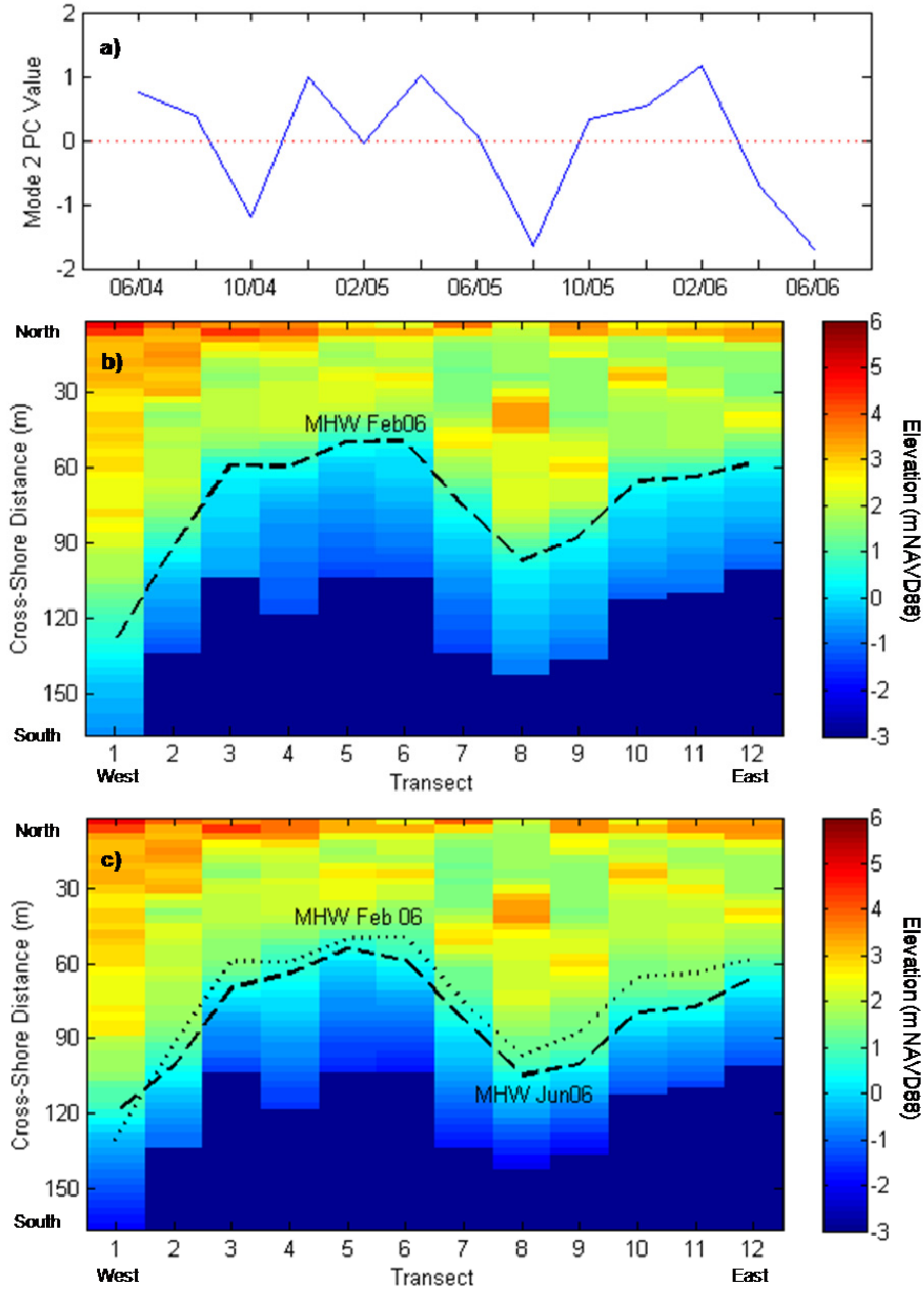

Figure 15. Fluctuations in beach topography exhibited by M2 between winter and summer. a) M2 PC time series. b) Map view M2 beach configuration at February 2006 PC value. c) Map view M2 beach configuration at June 2006 PC value. MHW = +0.55 m NAVD88.

predominantly in the summer, represent a seaward advance of the shoreline at transects 2-12 and a landward retreat at transect 1.

To test whether this annual periodicity was reflected in the surveyed shoreline, a regression analysis was conducted between the M2 PC and the mean cross-shore position of MHW measured during each survey. This relationship was significant ($p=0.047$) and negatively correlated ($r= -0.56$), indicating that increases in the PC value, occurring predominantly during winter months, reflected a landward retreat of MHW (Figure 16). Likewise, a decrease in the PC value, which occurred during summer months, indicated a seaward advance of MHW. Calculating a mean cross-shore position of MHW for all transects suppressed the inverse relationship identified at transect 1, but showed that a majority of the study area does exhibit this seasonal pattern.

To identify regions of high vertical variability for M2, vertical changes in elevation were measured from the highest PC value (February 2006), representing the maximum winter configuration, to the lowest PC value (June 2006), representing the maximum summer configuration (Figure 17). Two distinct bands of cross-shore variability occur between the winter and summer configurations. The seaward end of most profiles erode up to 1.5 m vertically (hotter colors) from winter to summer while a band further landward accretes up to 1.5 m vertically (cooler colors). This pattern indicates a cross-shore pivot point exists along these transects. Cross-section plots of the M2 beach profiles at the February and June 2006 PC values (Figure 18) reveal that a majority of transects (3, 5, 6, 8, 9, 10, 11, and 12) exhibit a cross-shore pivot point at MSL (-0.17 m NAVD88) between the two seasonal configurations where no vertical change occurs throughout the mode. From winter to summer, the beach face at these

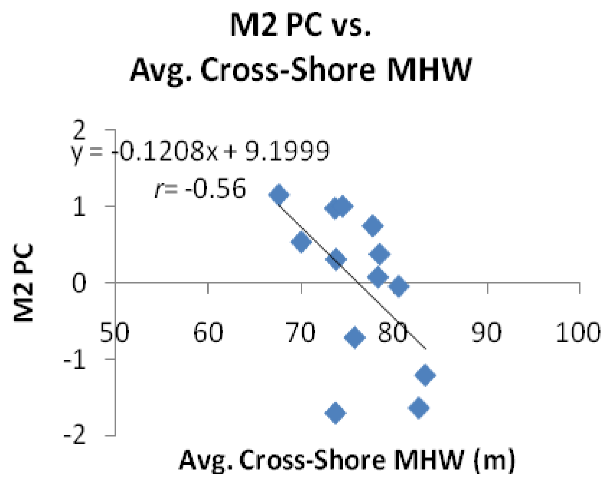

Figure 16. Correlation of the mean cross-shore position of MHW against the M2 PC.

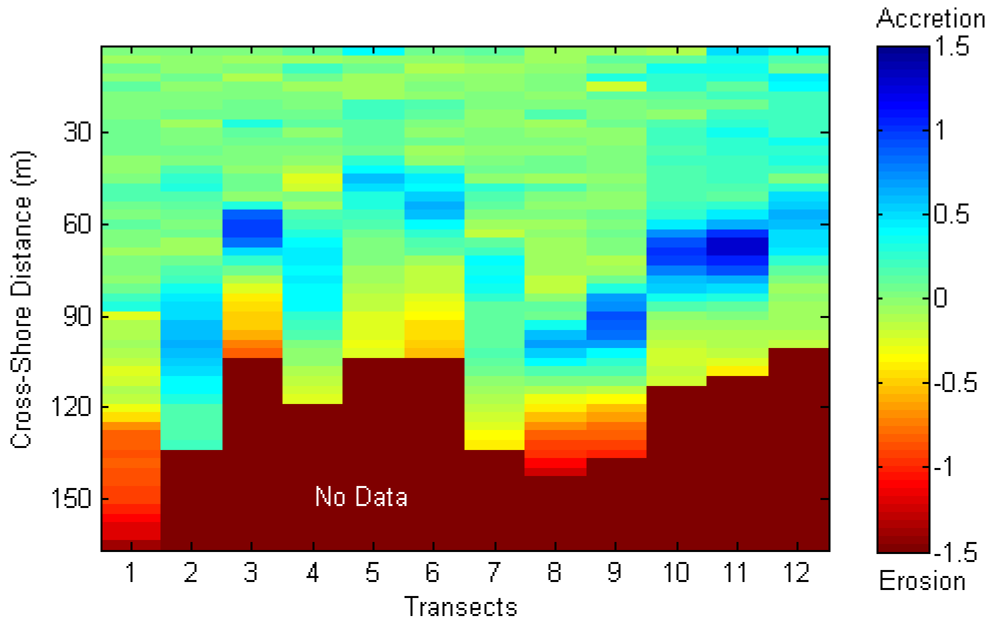

Figure 17. M2 vertical changes in elevation from winter (February 2006) to summer (June 2006). Cool colors represent gain in elevation from February to June and hot colors represent loss of elevation.

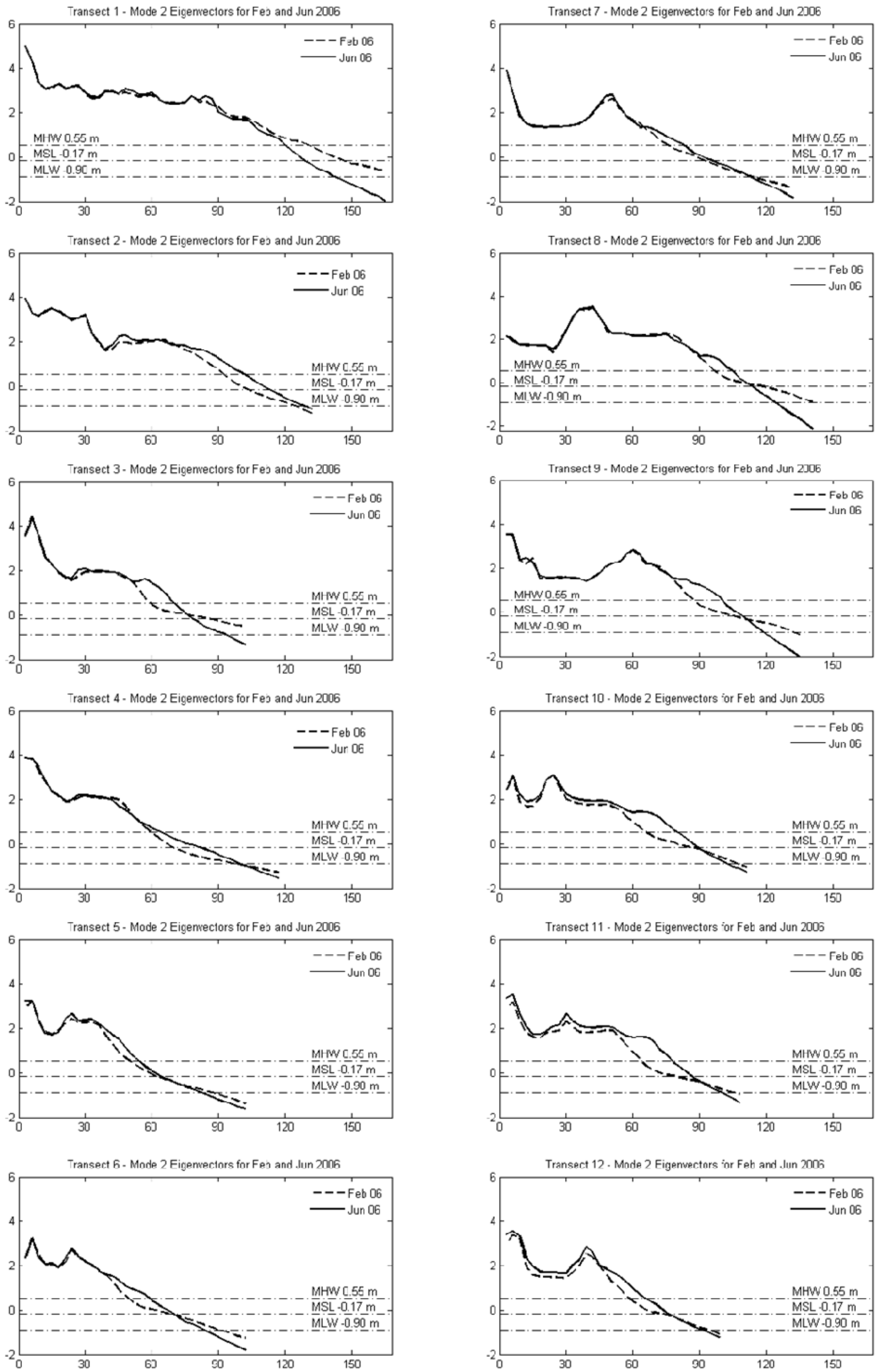

Figure 18. M2 beach profiles for each transect at maximum (February 2006) and minimum (June 2006) PC values.

transects accrete above MSL and erode below MSL. From summer to winter, the pattern is reversed with the beach face above MSL eroding and below MSL accreting. Transects 4 and 7 show a similar pattern with a cross-shore pivot point at MLW (-0.90 m NAVD88). Transect 1 shows erosion of the whole beach face from winter to summer while transect 2 shows accretion of the whole beach face over the same period. The inverse occurs at these transects from summer to winter.

Wave Climate and Water Level

Calculations of monthly mean and maximum values for wave and water level parameters are shown in Figures 19 and 20. Mean wave and water level parameters for the entire study period are shown in Table 3. In general, monthly mean values showed more seasonal regularity than maximum values. Fall months were the calmest with lower mean significant wave heights, steepness, and energy and higher mean wave periods and wave lengths. Mean wave direction was northward during the late summer and early fall months and slightly more easterly during the rest of the year. Spring months were characterized by higher significant wave heights and energy. The parameters showing the most seasonal regularity were mean observed water level and surge with peaks during September and October and minimum values in March and April. Monthly maximum wave and water level values showed little periodicity.

M1 Correlation with Wave and Water level Data

Mean and maximum wave and water level parameters measured over the day, week, and month before each survey as well as the entire period between surveys were correlated against the M1 PC to determine whether patterns of variability in beach topography described by M1 showed significant relationships with local wave and water

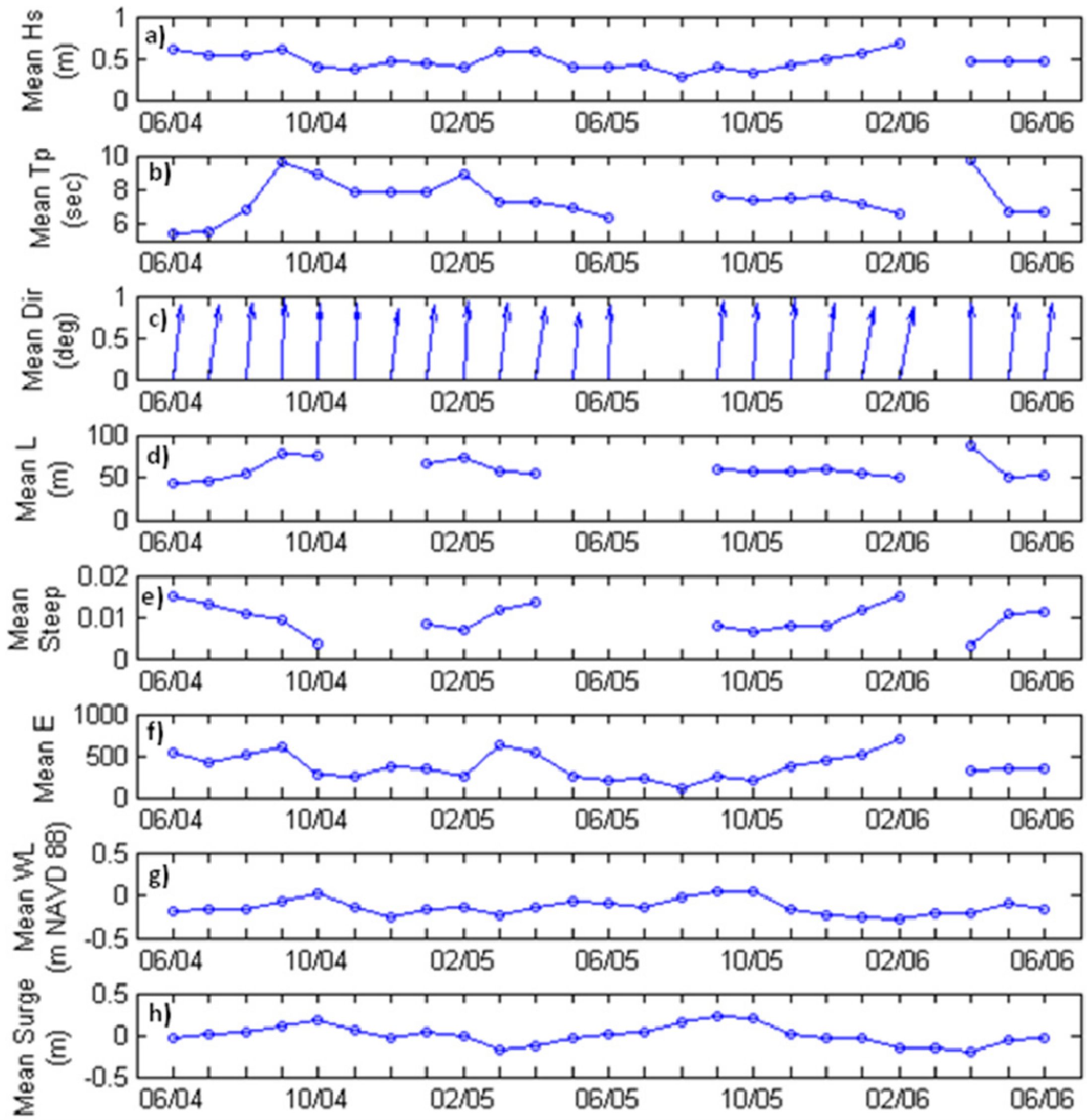

Figure 19. Monthly mean calculations of local wave and water level parameters from June 2004 to June 2006. a) significant wave height b) wave period c) wave direction d) wavelength e) wave steepness f) wave energy g) water level h) surge (observed – predicted water levels).

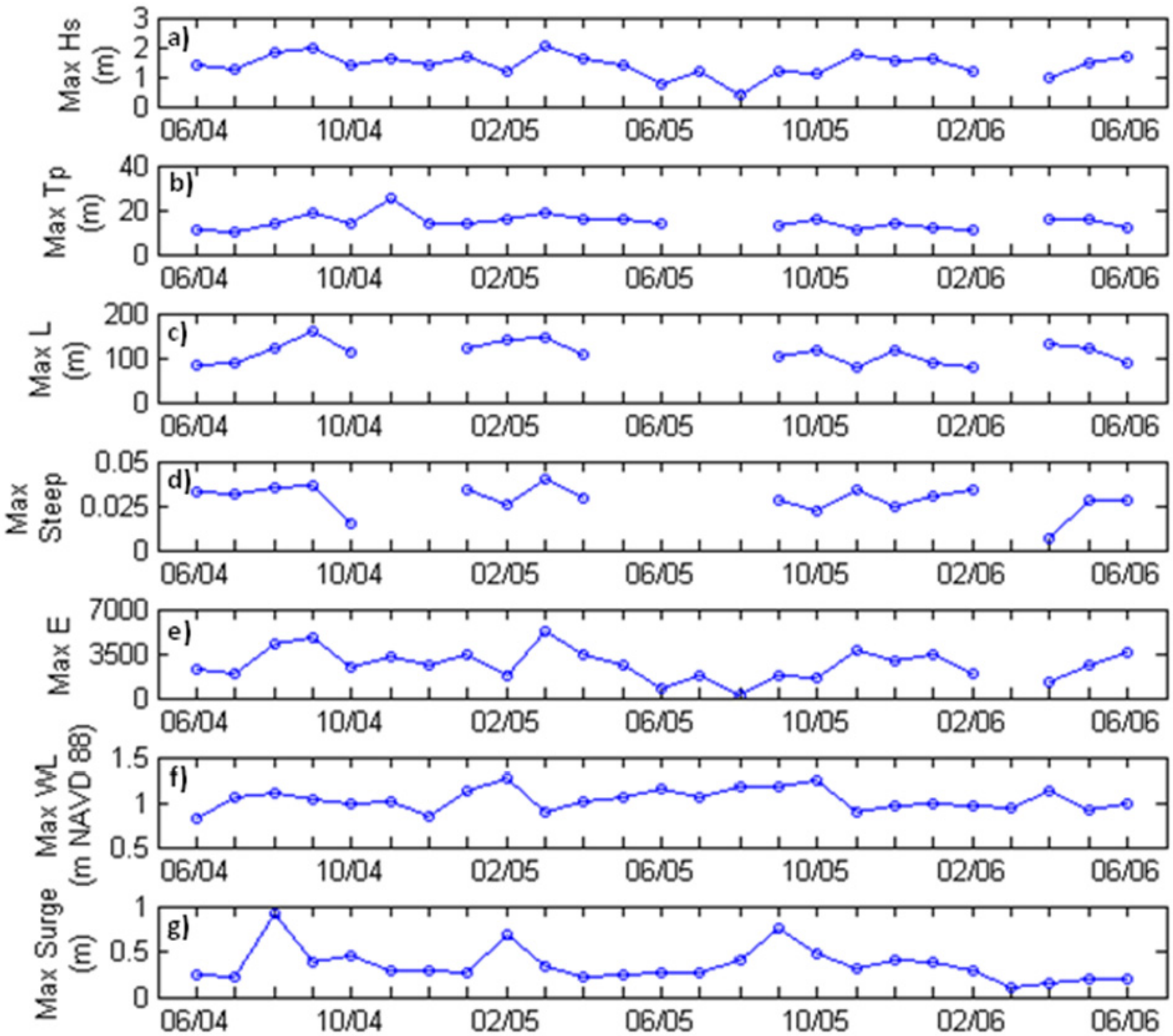

Figure 20. Monthly maximum values for local wave and water level parameters from June 2004 to June 2006. a) significant wave height b) wave period c) wavelength d) wave steepness e) wave energy f) water level g) surge (observed – predicted water level)

Parameter	Mean
Hs (m)	0.47
Tp (sec)	7.39
Dir (deg)	191.26
L (m)	57.74
Steepness	0.01
Energy	372.93
WL (NAVD88)	-0.14
Surge (m)	0.00

Table 3. Mean wave and water level parameters from June 2004 to June 2006.

level parameters (Table 4). No significant relationships between the M1 PC and any of the wave or water level parameters measured over different temporal scales were found. The M1 PC seems to more strongly reflect the mean shoreline position over the study duration which shifted from seaward to landward between August and December 2005. To test this hypothesis, the mean cross-shore position of MHW for all transects during each survey was calculated and then correlated against the M1 PC (Figure 21). These values were positively ($r = 0.80$) and significantly correlated ($p = 0.001$). Although no correlations between wave and water level parameters and the M1 PC were identified, the temporal and spatial pattern of variability exhibited by M1 does show a series of erosive events between August and December 2005.

M2 Correlation with Wave and Water level Data

To identify those processes causing the apparent seasonal variability reflected in the M2 PC, correlation analyses were conducted between the M2 PC and local wave and water level parameters (Table 5). These wave parameters were obtained over the same four time scales used to examine M1: the day, week and month before the survey as well as the period between surveys. The M2 PC was significantly and positively correlated with mean wave energy the month before the survey (r=0.61, p=0.035), mean Hs the month before the survey (r=0.59, p=0.043), and maximum Hs the week before the survey (r=0.65, p=0.044). Correlations between the M2 PC and wave parameters at both longer (intra-survey period) and shorter (day before survey) time scales showed no significant relationships ($p<0.05$). This finding indicates that the prevailing wave climate determined at temporal scales of between one week and one month before the survey is

Wave Parameters	1 Day Before Survey		7 Days Before Survey		30 Days Before Survey		Until Prior Survey (± 60 Days)	
	r	p	*r*	p	*r*	p	*r*	p
Mean Hs	0.32	0.358	0.25	0.475	-0.34	0.275	0.07	0.808
Maximum Hs	0.37	0.286	0.13	0.719	-0.28	0.377	-0.06	0.864
Mean Tp	-0.01	0.990	-0.02	0.958	0.18	0.605	0.12	0.706
Maximum Tp	-0.20	0.573	0.28	0.438	0.52	0.099	0.10	0.752
Mean L	-0.10	0.848	0.26	0.570	0.34	0.370	0.35	0.362
Maximum L	-0.23	0.666	0.24	0.600	0.46	0.216	0.27	0.487
Mean Steepness	0.50	0.308	0.13	0.782	-0.17	0.655	0.15	0.698
Maximum Steepness	0.73	0.102	0.16	0.753	0.33	0.361	0.43	0.242
Mean E	0.30	0.400	0.27	0.450	-0.38	0.222	0.01	0.970
Maximum E	0.38	0.282	0.17	0.647	-0.27	0.404	0.03	0.925
Mean Direction	0.12	0.741	0.10	0.780	-0.27	0.413	-0.14	0.661
Mean Surge	-0.08	0.805	0.02	0.955	0.30	0.319	0.16	0.590
Maximum Surge	-0.02	0.954	0.11	0.723	0.13	0.660	0.15	0.617
Mean Water Level	0.00	0.9802	0.03	0.929	0.41	0.164	0.19	0.528
Maximum Water Level	0.21	0.483	0.10	0.735	0.30	0.317	0.24	0.426

Table 4. Results of correlations between the M1 PC and local wave and water level parameters measured over four distinct time scales (significance at $p<0.05$). No significant correlations were found between the M1 PC and the local wave and water-level parameters identified.

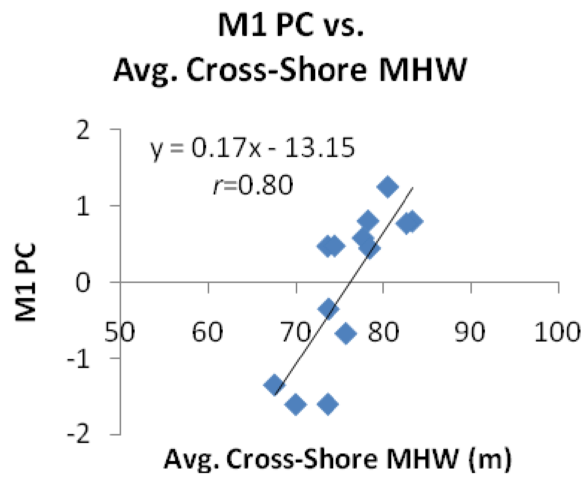

Figure 21. Correlation of the mean cross-shore position of MHW against the M1 PC.

Wave Parameters	1 Day Before Survey		7 Days Before Survey		30 Days Before Survey		Until Prior Survey ($\pm$ 60 Days)	
	r	p	*r*	p	*r*	p	*r*	p
Average Hs	0.40	0.249	0.54	0.106	**0.59**	**0.043**	0.35	0.266
Maximum Hs	0.40	0.249	**0.65**	**0.044**	0.27	0.401	0.17	0.595
Average Tp	0.03	0.938	-0.48	0.161	-0.18	0.591	-0.17	0.589
Maximum Tp	-0.12	0.739	-0.08	0.826	-0.21	0.536	0.19	0.557
Average L	0.20	0.709	-0.38	0.394	-0.40	0.282	-0.36	0.340
Maximum L	0.04	0.946	0.37	0.418	0.36	0.347	0.56	0.119
Average Steepness	-0.26	0.618	0.42	0.354	0.46	0.217	0.24	0.541
Maximum Steepness	-0.06	0.910	0.59	0.167	0.27	0.488	0.40	0.283
Average E	0.44	0.198	0.61	0.062	**0.61**	**0.035**	0.41	0.190
Maximum E	0.45	0.193	0.57	0.088	0.17	0.590	0.16	0.628
Average Direction	0.56	0.094	0.61	0.062	0.52	0.105	0.52	0.082
Average Surge	**0.69**	**0.008**	0.35	0.236	0.19	0.532	0.03	0.924
Maximum Surge	**0.61**	**0.028**	0.06	0.844	0.24	0.438	0.34	0.258
Average Water Level	**0.83**	**0.0004**	0.44	0.136	0.28	0.362	0.19	0.525
Maximum Water Level	0.46	0.110	0.19	0.538	0.10	0.752	0.03	0.914

Table 5. Correlations between the M2 PC and local wave and water level parameters measured over four distinct time scales ($p<0.05$ shows significant relationship).

more closely linked to the M2 pattern of variability in beach topography identified within the study area.

Correlations conducted between the M2 PC and water level parameters, however, showed significant relationships at much shorter time scales (Table 5). Out of all wave and water level correlations conducted for this mode, the most significant relationships were between the M2 PC and mean water level the day before the survey (r = -0.83, p = 0.0004), mean surge the day before the survey (r = -0.69, p = 0.008) and maximum surge the day before the survey (r = -0.61, p = 0.028). Each of these parameters was negatively correlated with the M2 PC indicating higher water levels and surge correlated with a summer beach configuration (low M2 PC values) while lower water levels correlated with a winter beach configuration (higher M2 PC values). In addition, three of the four water level parameters studied (mean surge, mean water level, maximum water level) showed decreasing significance with an increase in time scales. This result implies that short term variability in water level is more closely correlated to variability in beach topography described by this mode than conditions over longer time scales.

Wind Climate and Correlations with M1 and M2

Analysis of the local wind climate during the study period revealed seasonal patterns. Local wind direction rotated counterclockwise over the course of a year (Figure 22). In the summer, winds are weak and onshore, blowing to the north-northeast. During the early fall, winds blow strongly offshore to the southwest and then rotate toward the southeast in the winter. Finally during the spring, winds typically blow alongshore to the east. The wind rose of data from Frying Pan Shoals shows that during the duration of the study, winds blew predominantly from the southwest and north-northeast showing

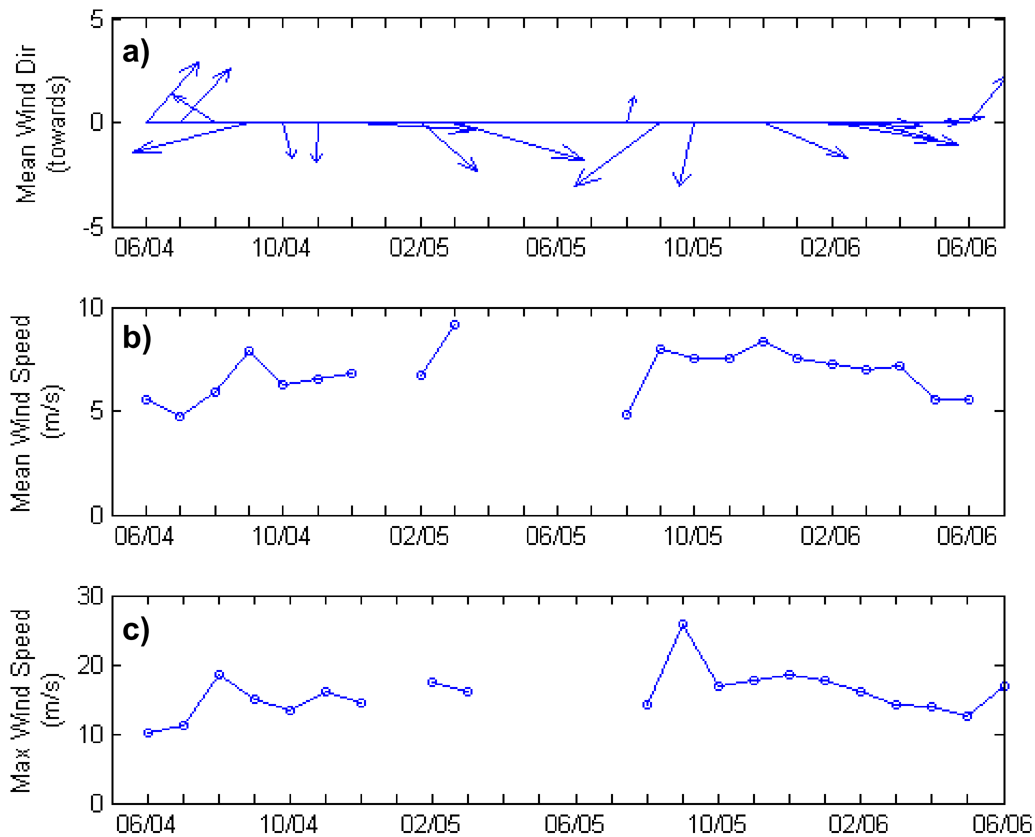

Figure 22. Monthly mean wind direction (a) and speed (b) and monthly maximum wind speed (c) from June 2004 to June 2006. Plot (a) indicates the mean direction wind is blowing towards.

seasonality in the local wind field (Figure 23). However, no significant correlations were detected between the M1 and M2 PCs and wind data collected (Table 6).

DISCUSSION

Two dominant modes of variability in beach topography were identified in the EOF analysis, and combined to describe 63% of the variability during the two year study period. These modes were distinct with the first mode (44%) reflecting large scale, storm driven variability occurring from August to December 2005 and the second mode (19%) reflecting smaller scale seasonal variability occurring throughout the duration of the study.

Storm Events

M1 identified a large-scale shoreline retreat along the entire study reach between the August and December 2005 beach profile surveys with all transects fluctuating in phase together. Correlation analyses between the M1 PC and local wave, water level, and wind parameters revealed no significant relationships. However, a potential explanation for the lack of correlation is the shape of the PC time series itself which shows a large shift in value from positive to negative between August and December 2005. An extreme event or series of events likely to drive the magnitude of shoreline erosion identified in M1 may appear as a spike in the record rather than a shift in values. The erosive impact of storms on North Carolina's barriers has been well documented (Komar, 1976; Birkemeier, 1984; Sallenger et al, 1985; Dolan and Davis, 1992). A combination of increased wind, waves and water levels during storms can lead to large scale erosion events, and in extreme cases, destruction of dunes and barrier island overwash. The first major storm to impact the study area from June 2004 to June 2006

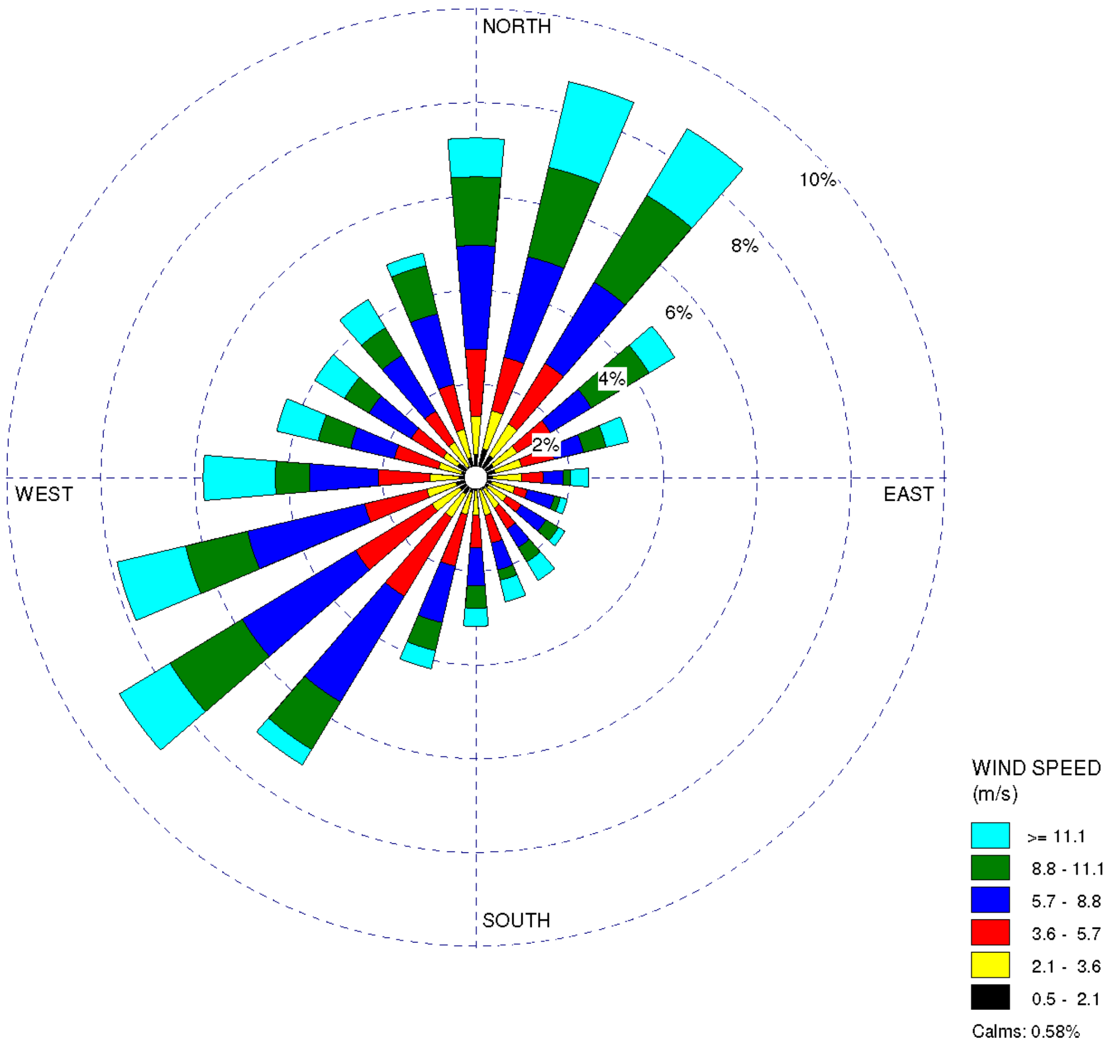

Figure 23. Wind rose for data from FPSN7 between June 2004 and June 2006 showing occurrence of direction and magnitude in which winds blew from.

Wind Parameters	1 Day Before Survey		7 Days Before Survey		30 Days Before Survey		Until Prior Survey (± 60 Days)	
	r	p	*r*	p	*r*	p	*r*	p
M1 PC								
Mean Speed	-0.37	0.256	-0.52	0.100	-0.50	0.114	-0.37	0.233
Maximum Speed	-0.16	0.640	-0.11	0.756	-0.55	0.082	-0.42	0.174
Mean Direction	0.39	0.232	0.20	0.558	-0.17	0.620	-0.18	0.566
M2 PC								
Mean Speed	0.48	0.136	0.56	0.0744	0.45	0.1678	0.53	0.0746
Maximum Speed	0.58	0.062	0.42	0.1996	0.28	0.4127	0.30	0.3456
Mean Direction	0.28	0.4031	0.20	0.5492	0.38	0.2483	0.37	0.2384

Table 6. Correlations between the M1 and M2 PCs and local wind parameters measured over four distinct time scales ($p<0.05$ indicate significance). No significant correlations were detected between wind data and either PC.

was Hurricane Charlie, which made landfall at Cape Romain South Carolina on the morning of August 14, 2004 as a weak Category 1 Hurricane. Peak wind gusts at Oak Island were measured at 34 m/s, and *Hs* measurements at station OKI peaked at 1.8 m on August 14 at 1300h (Figure 24). A maximum storm surge of approximately 1.6 m was recorded at Sunset Beach at 1200h on August 14 just before low tide (Figure 24). The surge was short lived, only lasting several hours. During this period minimal beach erosion occurred along Oak Island.

The 2005 Atlantic storm season was extremely active with a total of 27 named storms. The largest of these storms impacted the Florida and Gulf coasts; however, several storms impacted southeastern North Carolina. Wave parameters recorded from August to December 2005 are shown in Figure 25. Hurricane Ophelia passed through the Cape Fear region from September 12-14, 2005 as a Category 1 Hurricane. Peak wind gusts associated with Ophelia reached 35 m/s. From September 12-15, Brunswick County experienced heavy rainfall with Oak Island receiving the highest recorded total in the Cape Fear region at 44.5 cm. This led to extensive flooding on the island (NWS, 2008). Wave heights associated with Ophelia were elevated with a maximum *Hs* of 1.2 m recorded at Station OKI on September 14 at 1400h (Figure 26). Although wave heights recorded during the hurricane were not extraordinary, storm surge associated with Ophelia lasted for several days. The Sunset Beach tide station recorded a maximum storm surge of 0.84 m on September 13 during mid-tide at 1930h (NWS, 2008). Of the six high tides occurring from September 12-14, five showed observed water levels that exceeded predicted levels by 0.2-0.4 m (Figure 26). In addition, *Hs* measurements

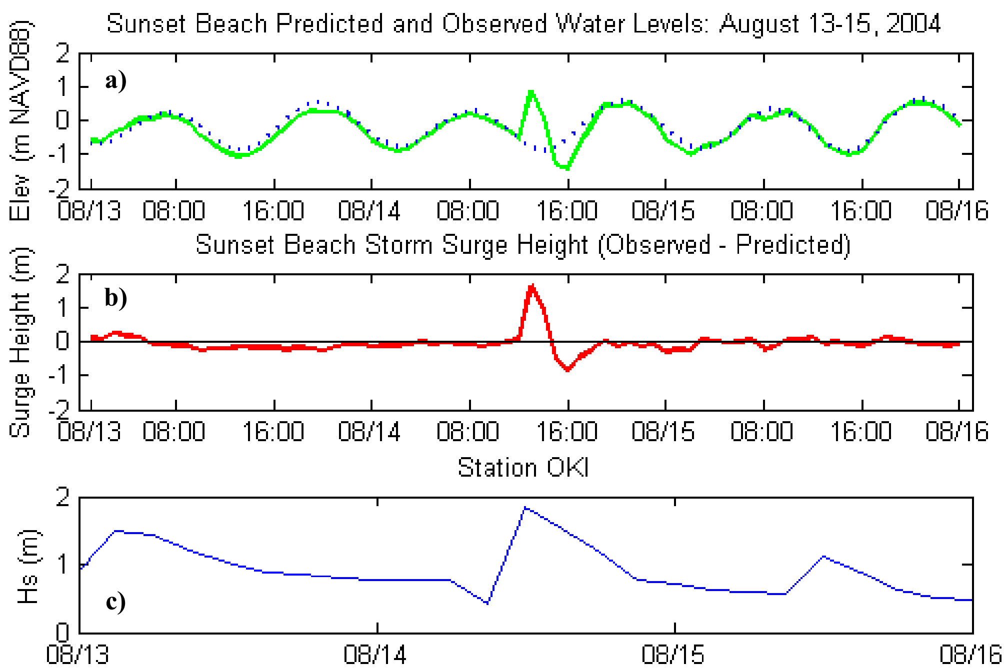

Figure 24. Local water levels and *Hs* recorded during Hurricane Charlie (August 13-15, 2004). a) predicted and observed water levels b) storm surge c) significant wave height.

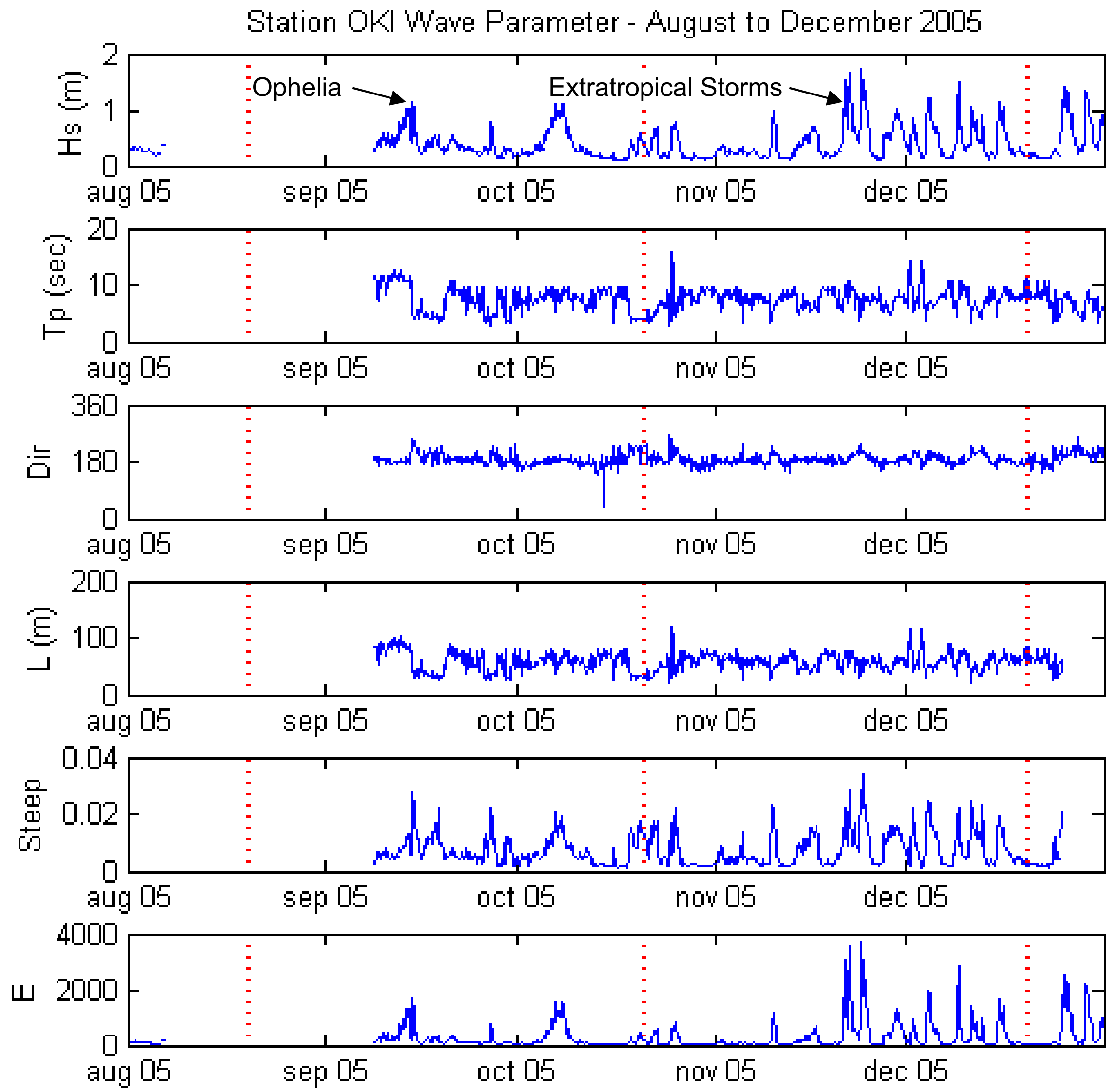

Figure 25. Local wave parameters from August through December 2005. Hurricane Ophelia passed through the Cape Fear region from September 12-14. Two strong extratropical storms passed through the region from November 21-24. Vertical red lines represent dates of beach profile surveys.

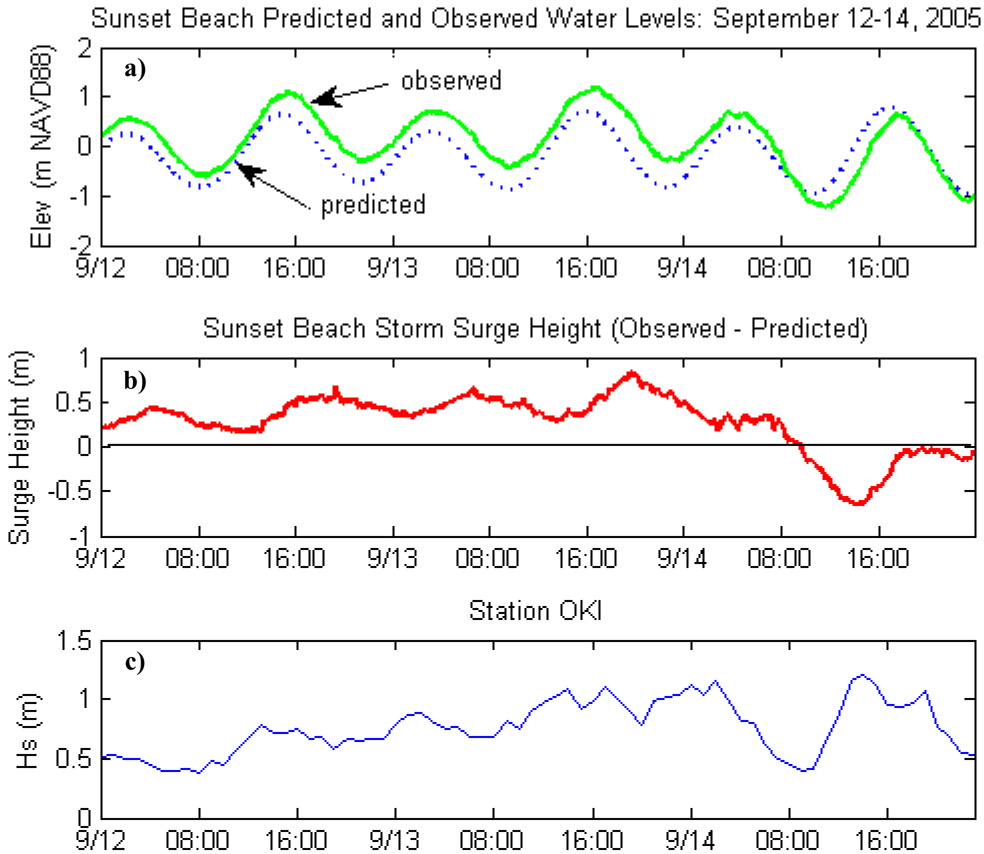

Figure 26. Local water levels and *Hs* recorded during Hurricane Ophelia (September 12-14). a) predicted and observed water levels b) storm surge c) significant wave height.

recorded at station OKI during these high tides ranged from 0.7-1.0 m (Figure 26). Beyond Hurricane Ophelia, water level observations at Sunset Beach show that during the two months prior to the October 2005 beach profile survey, the mean observed water level and storm surge was twice as high as it was during any other intra-survey period from June 2004 to June 2006 (Figure 27).

Several studies have found that the sum of astronomical tides and storm surge (dubbed "storm tides") can be more important in driving beach erosion during storms than waves (Edelman, 1972; Vellinga, 1982; Steetzel, 1991; Zhang et al., 2001; Pye and Blott, 2008). Storm tides allow waves to impact higher portions of the beach profile including the berm and dune, leading to increased rates of erosion. Pye and Blott (2008) found that the largest erosion events occurring along the Stefon coast in northwest England between 1958 and 2008 were associated with extreme high tide events (observed high tides 1 to 2 m above predicted high tides) and especially with successive extreme high tides. Oak Island is relatively low-lying with the beach berm located between 1.7 and 2.0 m above MSL. It is likely that extended storm tides and increased wave activity associated with Hurricane Ophelia played a dominant role in forcing shoreline retreat identified in M1 between August and October 2005.

The M1 PC fluctuates further negative from October to December 2005 showing continued landward retreat of the shoreline. Inspection of the wave record during this time period shows a pair of high energy events with elevated wave heights during late November 2005 (Figure 25). These events were strong extratropical Category 1 storms based on the Dolan and Davis categorization (1996) which classifies extratropical storms by wave height and storm duration. Each of these storms was accompanied by strong

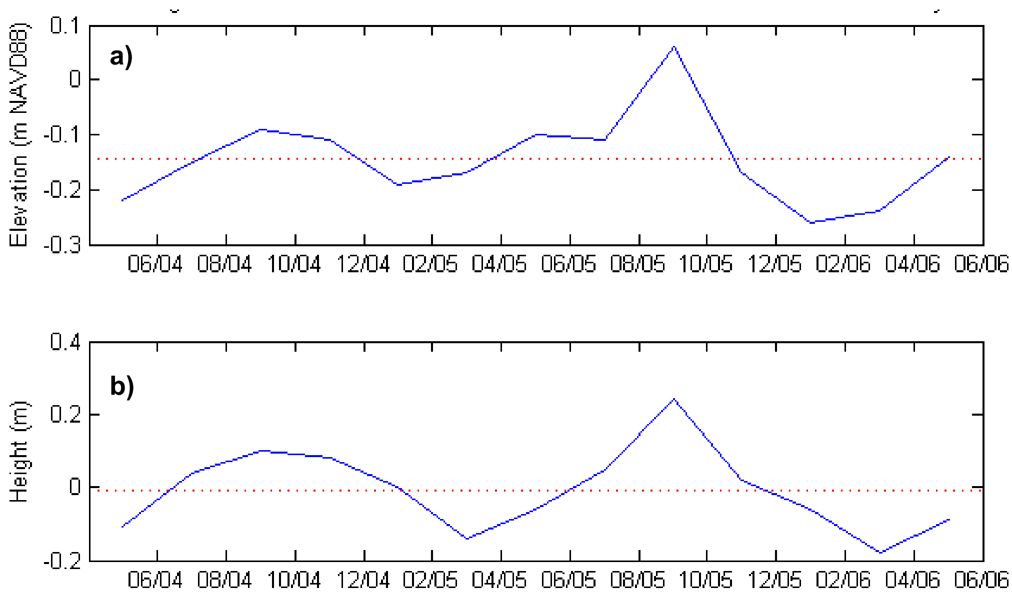

Figure 27. Mean water level observations (a) and observed minus predicted observations (b) at Sunset Beach between each beach profile survey from June 2004 to June 2006.

onshore winds. The first event formed from a stationary warm front in the Gulf of Mexico that tracked northeast and impacted the study area from November 21-22, 2005 (Davis et al, 2006). A maximum *Hs* of 1.7 m was recorded for this event at Station OKI on November 22 at 0400h (Figure 28). Storm surge peaked at 0.6 m on November 21 at 0930h. This surge approximately coincided with high tide and was accompanied by a *Hs* of 1.4 m as measured at Station OKI (Figure 28). The second November event formed from the convergence of a Canadian cold front and a low pressure system east of the Great Lakes (Davis et al, 2006) and impacted the study area from November 23-24, 2005. Wave heights recorded at station OKI during this storm peaked at 1.7 m on November 24 at 0100h (Figure 28). No significant storm surge accompanied this event.

From October to December of 2005, MHW retreated landward an average of 2.9 m. However, shoreline movement was much more variable than patterns observed between August and October 2005. At transect 1, MHW retreated landward 19.3 m. The remainder of the study area showed smaller signs of storm impact with some areas even showing seaward accretion (Table 2). Previous studies have shown that patterns of variability in EOF analyses can sometimes be influenced by isolated areas of large variability (Haxel and Holman, 2004; Miller and Dean, 2007). Although M1 shows similar retreat of the shoreline from October to December 2005 as that identified from August to October 2005, this is likely due to the large amount of shoreline retreat which occurred at transect 1. Similar to Hurricane Charlie, the two extratropical storms occurring in late November 2005 exhibited higher significant wave heights than

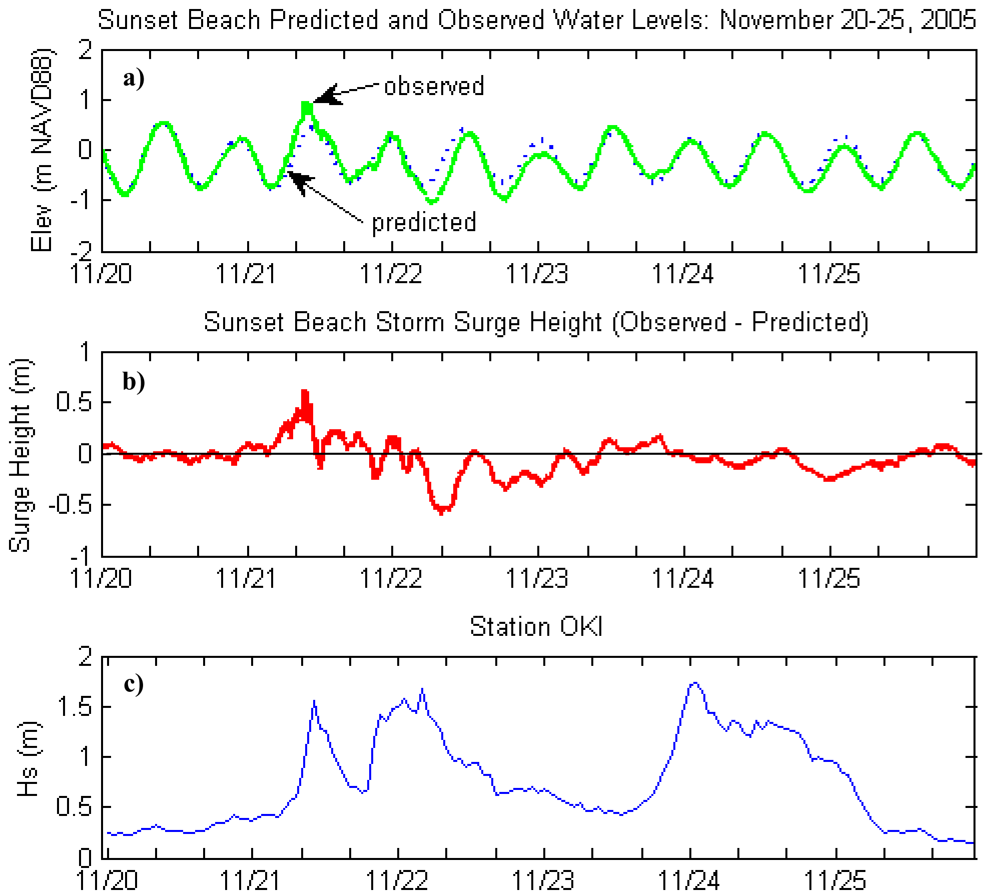

Figure 28. Water levels and *Hs* recorded during two successive extratropical storm events in November 2005. a) predicted and observed water levels b) storm surge c) significant wave height.

Hurricane Ophelia but had a much shorter storm surge which was isolated to one elevated high tide. Thus, shoreline erosion was much less extensive during this period. High rates of shoreline retreat at transect 1, which lies adjacent to Lockwood's Folley Inlet, could have been forced by inlet dynamics in addition to increased water levels and storm waves associated with the November storm events. In similar settings in North Carolina and Florida, fluctuations in inlet channel geometry and subsequent migration of ebb tidal deltas have been shown to heavily influence shoreline variability adjacent to inlets. Ebb deltas associated with tidal inlets provide some wave sheltering to the landward beach (Cleary, 1996; Fitzgerald, 1996; Davis and Barnard, 2003). If an ebb delta shifts laterally, portions of the beach previously protected by the ebb delta may be exposed and experience increased rates of erosion. The opposite may occur when an ebb delta migrates laterally in front of a beach not previously protected by an ebb delta. This may very well be occurring at Lockwood's Folley Inlet. Thus, variability in beach topography described by M1 was likely forced predominantly by storm tides and wave activity associated with Hurricane Ophelia, with additional forcing by subsequent extratropical storms and inlet influence.

Seasonal Variability of Beach Topography and Forcing

M2 was shown to exhibit small-scale, seasonal periodicity with transect 1 fluctuating out of phase with the remainder of the transects. For transects 2-12, M2 exemplified seasonal cycles of cross-shore sediment transport that have been observed in other studies (Winant et al., 1975; Komar, 1976; Aubrey, 1979; Birkemeier, 1984; Larson and Kraus, 1993). These studies showed a close relation between seasonal fluctuations in beach topography and seasonal fluctuations in wave climatology. Higher wave heights and wave energy during the winter months tended to scour sediment from the beach and force movement of sediment seaward, while lower wave heights and wave energy during the summer and early fall tend to allow sand to move landward to the beach through longer period swell (Winant et al, 1975; Aubrey, 1979; Lee et al., 1998). The local wave climate in Long Bay did exhibit seasonal fluctuation during the study period with higher mean wave heights and energy in the winter months and calmer conditions in the summer months. Mean significant wave height and mean wave energy the month before each survey showed significant correlations with the M2 PC, as did the maximum significant wave height the week before the survey. Correlations between the M2 PC and these wave parameters suggest seasonal variability in beach topography along Long and Yaupon beaches may be linked to seasonal variability in the wave climate. The fact that these parameters do not correlate with the M2 PC when averaged over a daily window suggests that short-term variability in the wave climate occurs throughout the year and may not drive seasonal change in beach topography exhibited by M2. This finding suggests seasonal variability in beach topography identified by M2 may be driven more by average conditions that prevail over longer periods of time. Large-scale, short term events such as storms were found to be more closely linked to patterns of variability identified in M1.

It is unclear why transect 1 is showing a reversal in the typical seasonal pattern of cross-shore sediment transport, with the beach face eroding from winter to summer and accreting from summer to winter. The entire beach surface below the berm crest at transects 1 and 2 fluctuates out of phase with each other, indicating the possibility of an along-shore exchange. The wave data showed some seasonal variability in direction with fluctuations between northward and north-northeastward during the study. Waves tend to approach in a more northward direction during the late summer and early fall and shift eastward in the winter. This fluctuation in wave direction could potentially setup seasonal variability in along-shore transport direction. Davis (2005) identified eastward dominated subtidal currents along the shelf using current data from station OKI located in approximately 7 m water depth. There is a possibility that this current extends to shallower depths and could be influencing alongshore sediment transport, however, this is unknown. The inverse seasonal pattern observed at transect 1 could also be related to inlet dynamics operating at similar, seasonal time scales as that identified in M2. However, an analysis of potential forcing by inlet dynamics is outside the scope of this research.

M2 showed that the majority of transects in this study (transects 3-10) exhibited cross-shore pivot points between seasonal profiles from MSL and MLW. Pivot points between seasonal profiles also were identified by Aubrey (1979), who conducted an EOF analysis on five years of beach and nearshore profile data from Torrey Pines Beach, California. He identified cross-shore pivot points between seasonal profiles at 2-3 m below MSL and at 6 m below MSL. Aubrey (1979) hypothesized that wave height and tidal range played a role in the location of the pivot point but did not further analyze mechanisms of forcing.

An unexpected result of this research was high negative correlations between the M2 PC and water level parameters calculated over the shortest averaging windows. In fact, correlations between the M2 PC and mean water level, mean surge as well as maximum surge the day before each beach profile survey showed higher correlations than any other relationships tested in this study. This relationship shows an increase in water levels and surge the day before a survey correlating to a decrease in the M2 PC value, and thus a seaward accretion of transects 2-12 (landward erosion of transect 1). Previous research identified the opposite relationship with positive correlations between water levels and shoreline retreat at very short response intervals (Edelman, 1972; Vellinga, 1982; Steetzel, 1991; Zhang et al., 2001; Pye and Blott, 2008). In addition, this study found that water level parameters measured over increasingly longer averaging windows show decreasing correlation (apart from maximum surge) with the seasonal fluctuation of beach topography exhibited by M2. This suggests that the response interval between water level and the M2 pattern of variability is very short, however, the temporal spacing of the surveys did not allow closer investigation of this relationship.

Management Implications

Throughout North Carolina, regions of the coast in proximity to tidal inlets have been delineated as "Inlet Hazard Areas (IHA)" by the North Carolina Division of Coastal Management (DCM) and are listed as Areas of Environmental Concern (AEC). Under state law, these areas are defined as "natural-hazard areas that are especially vulnerable to erosion, flooding and other adverse effects of sand, wind, and water because of their proximity to dynamic ocean inlets" (15A NCAC 07H .0304). Within these areas, there are limits on the size of structures that can be built as well as increased oceanfront setbacks for structures. These zones were first developed in 1979 through inspection of aerial photography and determination of historical shoreline trends (Warren et al., 2007). The delineated zones were meant to stand for ten years, after which the zones would be re-examined and either expanded or minimized based on observed shoreline trends.

Nineteen years after the original expiration date, the IHAs have yet to be updated. Proposed plans to expand these areas have recently been released by the DCM but have not yet been adopted.

On the western end of Oak Island, in proximity to Lockwood's Folley Inlet, the current oceanfront limits of the IHA lies between transects 1 and 2 (shown in blue; Figure 29). The proposed IHA would expand the limits approximately 900 m eastward, between transects 2 and 3 (shown in red). In this study, the dominant pattern of variability in beach topography (M1, 44%) showed the highest vertical variability occurring along Long and Yaupon Beaches at transects 1 and 2, both of which lie in the IHA. These transects also experienced the largest rates of landward retreat within the study area. Although the duration of this study covered a relatively short timescale, the results support inclusion of the oceanfront beach at transect 2 in the IHA and adoption of the expanded zone to some point between transects 2 and 3. Because the proposed IHA extends its current limits to a point between transects 2 and 3, this study supports adoption of the newly proposed IHA.

CONCLUSIONS

An EOF analysis of bimonthly beach profile surveys along Oak Island, North Carolina revealed two dominant modes of variability in beach topography from June 2004 to June 2006. The first mode accounted for 44% of the total variability and reflected storm-driven shoreline change between August and December 2005. Extended storm surge and increased wave heights during Hurricane Ophelia and subsequent extratropical storms were identified as likely forcing agents for this mode which showed the shoreline did not recover to its pre-August 2005 position after these events. The

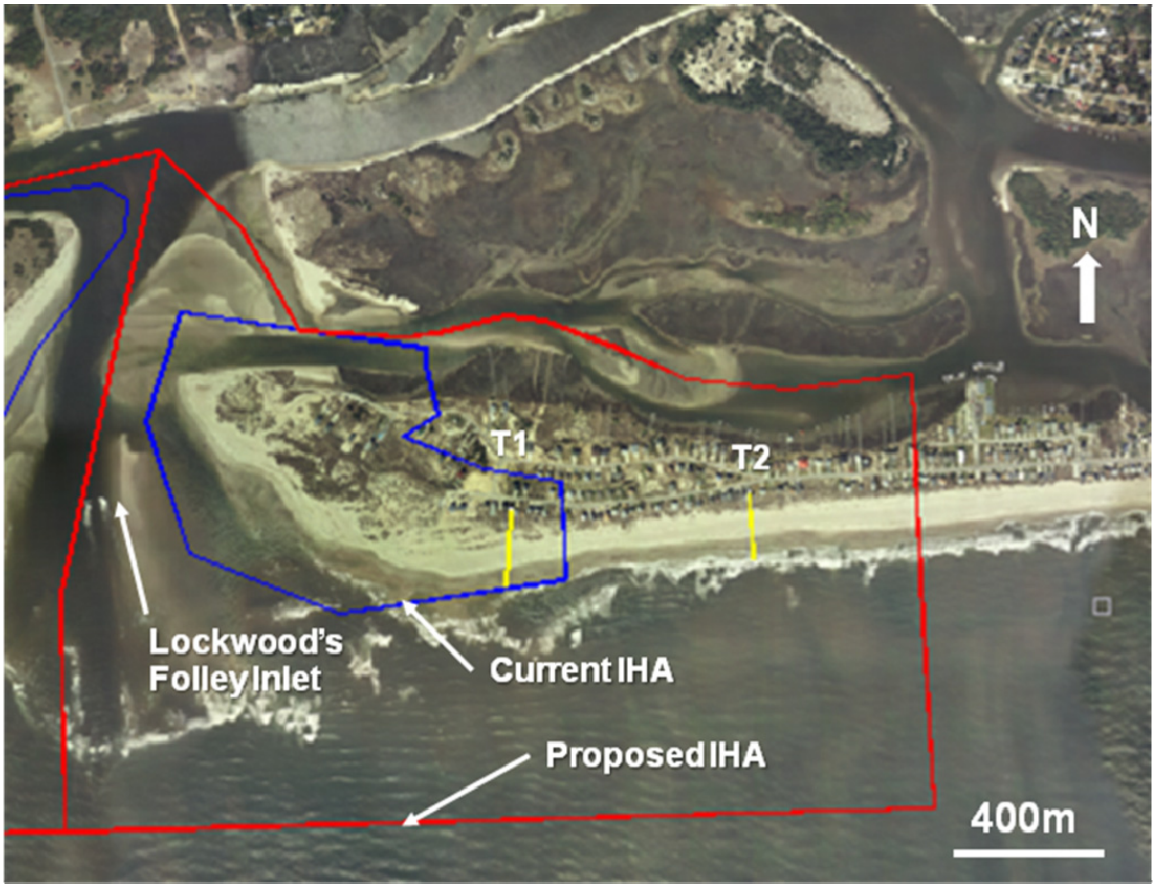

Figure 29. Location of current and proposed Inlet Hazard Areas (IHA) on the western end of Oak Island adjacent to Lockwood's Folley Inlet.

second mode exhibited smaller-scale seasonal fluctuations in beach topography and accounted for 19% of total variability. These seasonal patterns correlated well with significant wave height and wave energy measured over week to month averaging windows before each survey. A pivot point from MSL to MLW between winter and summer configurations was identified for a majority of transects. From winter to summer, transects 2-12 showed movement of sediment landward and then seaward from summer to winter. Transect 1 exhibited an inverse seasonal pattern with seaward transport from winter to summer and landward transport from summer to winter. The out-of-phase fluctuation of this transect with the rest of the study area indicates seasonal along-shore fluctuations of sediment transport which was proposed to be linked to seasonal changes in wave direction, subtidal currents, and possibly inlet dynamics. This study was found to have management applications and supported adoption of the newly proposed IHA in proximity to Lockwood's Folley Inlet which expands the IHA eastward to a point between transects 2 and 3.

REFERENCES

(In Format Required by *Estuarine, Coastal and Shelf Science*)

Aubrey, D.G., 1979. Seasonal patterns of onshore/offshore sediment movement. Journal of Geophysical Research. 84(C10), 6347-6354.

Aubrey, D.G., Ross, R., M., 1985. The quantitative description of beach cycles. Marine Geology. 69, 155-170.

Birkemeier, W.A., 1984. Time scales of nearshore profile changes. In: Proc. 19th International Conference on Coastal Engineering '84. ASCE, Houston, pp. 1507-1521.

Cleary, W.J., 1996. Inlet induced shoreline changes: Cape Lookout – Cape Fear. In: W.J. Cleary (ed.), Environmental Coastal Geology: Cape Lookout to Cape Fear, NC, North Carolina: Carolina Geological Society, pp. 49-59.

Cleary, W.J., McLeod, M.A., Rauscher, M.A., Johnston, M.K., Riggs, S.R., 2000. Beach nourishment on hurricane impacted barriers in southeastern North Carolina, USA: Targeting shoreface and tidal inlet sand resources. Journal of Coastal Research, ICS 2000 Proceedings. 232-255.

Cleary, W.J., Budde, L.E., 2005. Shoreline changes and beach monitoring along Oak Island, NC: Report prepared for the Town of Oak Island. 58 pp.

Cleary, W.J., Hasbrouck, E.G., 2006. Shoreline changes and beach monitoring along Oak Island, NC: Report prepared for the Town of Oak Island. 57 pp.

Crosby, D.S., Breaker, L.C., Gemmill, W.H., 1993. A proposed definition for vector correlation in geophysics: Theory and Application. Journal of Atmospheric and Oceanic Technology. 10(3), 355-367.

Davis, R.A., Barnard, P., 2003. Morphodynamics of the barrier-inlet system, west-central Florida. Marine Geology. 200, 77-101.

Davis, L., 2006. Hydrography and bottom boundary layer dynamics: Influence on inner shelf sediment mobility, Long Bay, NC. Master's Thesis. University of North Carolina Wilmington. 64 pp.

Dolan, R., Hayden, B.P., Lins, H., 1980. Barrier Islands. American Scientist. 68(1), 6-25.

Dolan, R., Davis, R.E., 1992. An intensity scale for Atlantic coast Northeast storms. Journal of Coastal Research. 8, 840-853.

Edelman, T., 1972. Dune erosion during storm conditions. Proceedings of the 11th

Conference of Coastal Engineering. 1305-1312.

Emery, W., and Thomson, R., 1997. Data Analysis in Physical Oceanography. Pergamon Press, Tarrytown, NY, 634 pp.

Fitzgerald, D.M., 1996. Geomorphic variability and morphologic and sedimentologic controls on tidal inlets. Journal of Coastal Research. 23, 47-71.

Haxel, J.H., Holman, R.A., 2004. The sediment response of a dissipative beach to variations in wave climate. Marine Geology. 206, 73-99.

Hoffman, C.W., Grosz, A.E., Nickerson, J.G., 1999. Stratigraphic framework and heavy minerals of the continental shelf of Onslow and Long Bays, North Carolina. Marine Georesources and Geotechnology. 17, 173-184.

IPCC, 2007: Climate Change 2007: Synthesis Report. Contribution of Working Groups I, II and III to the Fourth Assessment Report of the Intergovernmental Panel on Climate Change [Core Writing Team, Pachauri, R.K and Reisinger, A. (eds.)]. IPCC, Geneva, Switzerland, 104 pp.

Komar, P.D., 1976. Beach Processes and sedimentation. Prentice-Hall, Inc., New Jersey, 429 p.

Li, Y., Lark, M., Reeve, D., 2005. Multi-scale variability of beach profiles at Duck: A wavelet analysis. Coastal Engineering. 52, 1133-1153.

Larson, M., Hanson, H., Kraus, N.C., Newe, J., 1999. Short- and long-term responses of beach fills determined by EOF analysis. Journal of Waterway, Port, Coastal, and Ocean Engineering. 125(6), 285-293.

Miller, J.K., Dean, R.G., 2007. Shoreline variability via empirical orthogonal function analysis: Part I temporal and spatial characteristics. Coastal Engineering. 54, 111-131.

Miller, J.K., Dean, R.G., 2007. Shoreline variability via empirical orthogonal function analysis: Part II relationship to nearshore conditions. Coastal Engineering. 54, 133-150.

National Weather Service (NWS) Forecast Office. Hurricane Ophelia Weather Data. Accessed September 10, 2008. http://www.erh.noaa.gov/ilm/archive/09-14-05/index.shtml

Oertel, G.F., 1988. Processes of sediment exchange between tidal inlets and barrier islands. In: Aubrey, D.G., Weishar, L. (eds.), Hydrodynamics and sediment dynamics of tidal inlets, New York: Springer-Verlag. ASCE, pp. 186-225.

Pye and Blott, 2008 in press. Decadal-scale variation in dune erosion and accretion rates: An investigation of the significance of changing storm tide frequency and magnitude on the Sefton coast UK. Geomorphology.

Pfaff, S., 2008. Personal Communication.

Priesendorfer, R.W., 1988. Principal component analysis in meteorology and oceanography. New York, NY: Elsevier Science. 425 pp.

Snyder, S.W., Hine, A.C., Riggs, S.R., 1982. Miocene seismic stratigraphy, structural framework, and sea-level cyclicity, North Carolina continental shelf. Southeastern Geology. 23(4), 247-266.

Snyder, S.W., Hoffman, C.W., Riggs, S.R., 1994. Seismic stratigraphic framework of the inner continental shelf: Mason Inlet to New Inlet. North Carolina. North Carolina Geological Survey Bulletin No. 96. 59 p.

Steetzel, H.J., 1991. A model for profile changes during storm surges. Coastal Sediments '91. 618-630.

Vellinga, P., 1982. Beach and dune erosion during storms. Coastal Engineering. 6, 361-387.

Wallace, J.M., Dickenson, R.E., 1972. Empirical orthogonal representation of time series in the frequency domain. Part 1: Theoretical considerations. Journal of Applied Meteorology. 11(6), 887-892.

Wijnberg, K.M., Terwindt, J.H.J., 1995. Extracting decadal morphological behavior from high-resolution long-term bathymetric surveys along the Holland coast using eigenfunction analysis. Marine Geology. 126, 301-330.

Winant, C.D., Inman, D.L., Nordstrom, C.E., 1975. Description of seasonal beach changes using empirical eigenfunctions. Journal of Geophysical Research. 80 (15), 1979-1986.

Zhang, K., Douglas, B.C., Leatherman, S.P., 2001. Beach erosion potential for severe nor'easters. Journal of Coastal Research.